

MSc final-year project

A short analysis of the

Madden-Julian oscillations

Submitted by

ROCHETIN NICOLAS (rochetin.nicolas@hotmail.fr)

Under the guidance of
Prof G.S. BHAT

C.A.O.S LABORATORY (CENTRE FOR ATMOSPHERIC AND OCEANIC SCIENCES)
INDIAN INSTITUTE OF SCIENCES,
BANGALORE-560012
INDIA

Abstract

The Madden-Julian Oscillations (MJO) over the Indian and Pacific Ocean, are typically tracked by the anomalies of Outgoing Long-wave Radiation (OLR) and 850hpa winds (Zhang, 2005). It looks necessary for permitting the MJO eastward propagation from the equatorial Indian Ocean through the central Pacific Ocean beside the date line to have a background of westerly surface winds within a thin band 5°S - 5°S over the equatorial Indian Ocean and the Indonesian archipelago. Deep convection zones over Indian subcontinent during boreal summer and over western Pacific and northern Australia during austral summer appear to maintain the westerly winds throughout the year over the equatorial Indian Ocean. Indeed, in the case of an ENSO event (El Nino and Southern Oscillation), this background of westerlies disappears and we cannot see any MJO.

Signature of MJO has not been explored in moist static energy (h) yet. It is the sum of thermal energy ($C_p \cdot T$), latent heat ($L_v \cdot q$) and potential energy ($g \cdot z$) and gives the total energy of a unit mass of air neglecting the kinetic energy. In this work h at 500hpa level (mid-troposphere) is taken as the variable of interest. By using a simple wavelet analysis and FFT transform in Matlab, after normalisation by the red noise, we could notice that in case of strong MJO event, the variance of moist static energy at 500hpa over central Africa is also strengthened although this region is not recognized to be crossed by the MJO which is typically set up over the central Indian ocean. In some cases we can see in the time-power spectra of h at 500hpa a kind of resonance profile between central Africa, Indian Ocean and Indonesian archipelago. Moreover in many cases of strong and also weak MJO we observe a peak of moist static energy at mid-troposphere over Africa about 2 to 3 weeks before the peak observed over the two other regions. That time lag corresponds to a non dispersive wave phase speed between 3 and 6 m/s, which is in the recognized range of MJO propagation speed. Then we can suspect that a burst of convection over Africa might trigger an eastward moving wave like disturbance i.e an MJO event.

1. Introduction:

1.1. Definition:

Madden and Julian discovered in 1971 large amplitude oscillations in surface pressure and zonal winds in the tropical atmosphere having peak between 40 and 50 days. Now this mode of variation of the tropical atmosphere is called Madden-Julian Oscillation (MJO). Now MJO is recognized by the great majority of the experts in the tropics as one of the most important phenomena related with the variability of climate in the inter-tropical belt.

The observation of the variability of great inter-tropical phenomena compared simultaneously with MJO observation revealed several important associations (Zhang, 2005) e.g.,

- Strengthening of alizees winds over northern Brazil during strong MJO events and their weakening in the opposite case.
- The role of MJO in the triggering and propagation of tropical cyclones.
- MJO influences south Asian and north Australian monsoon variability. More in particular the prominent dries observed during very weak MJO and very important flood noticed in the opposite case.

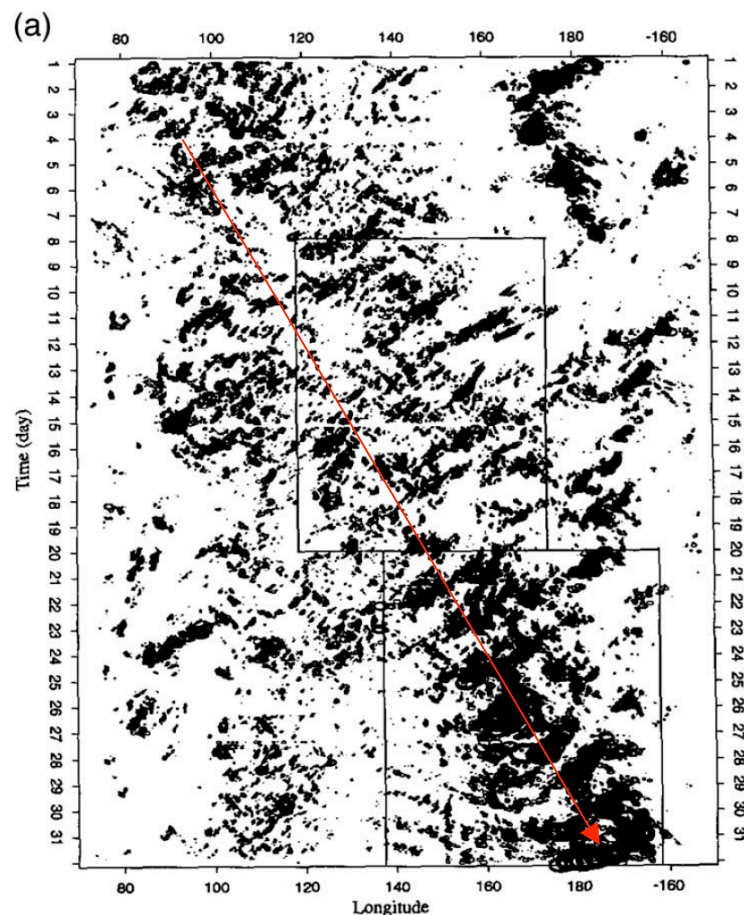


Figure 1 : Time-longitude diagram of convective cloud systems (black filled zones correspond to cloud top troposphere temperatures lower than 208 K) averaged in a band between 10°S-EQ from the 1st to the 31th of December 1992; at any given time, clouds are observed at different longitudes, but superposed on this and eastward migration of clouds is observed as indicated by a red arrow (Zhang, 2005)

Those correlations haven't been theoretically established yet, but observational evidences are sufficiently strong to allow the climatologists to assume a relationship between MJO and the above described phenomenon.

An MJO can typically be described as a planetary scale equatorial wave (wavelet order of 20 thousand km) of whom the period varies from 40 to 50 days with a spectral peak at 45 days. It is always associated with large scale deep convective clouds. More concretely, this wave on the whole, materialises itself by a convective cloud systems (Super Cloud Cluster, SCC) resulting in strong precipitations spread over several thousand kilometres and moving eastward at an average speed of 5 m/s inside a band 15°S-15°N, typically from the central Indian Ocean (60°E) up to the central Pacific Ocean (160°W) where it dissipates. This system of clouds is followed on its west side by a large field of high surface pressures and dry air. In fact this eastward movement is so prominent that it can be observed without any filtering method ([fig 1](#)).

However, the questions about its eastward propagation and periodicity haven't been fully explained theoretically by the scientists. The mechanism of this phenomena remains in a great part understood, although some very recent models just begin to reproduce good enough the complex structure of the MJO and their phase speed.

1.2. Observations:

- The most important pattern which has been noticed is the presence of strong westerlies in the lower troposphere qualified as “westerly winds anomaly”.
- In addition we can notice that an MJO event can be divide into two phases:
 - A so called **active phase** in which can be seen deep convection, heavy precipitations and increased westerly winds at the surface.
 - An **inactive phase**, during which mainly subsident motions and clear sky conditions dominate.

Finally we can say that the SCC is situated in a strong surface-wind-convergence zone.

- Wavelength:

The wavelength of the MJO is about 20000 km, thus we can speak about a planetary scale wave ([fig.2](#))

- Periodicity:

We typically describe the MJO period as being intraseasonal, that means less than a season and typically in 40 to 50 days with an occurrence peak at 45 days ([fig.3](#))

- The MJO structure:

In fact, the MJOs cannot be described properly as being equatorial sinusoidal waves, the propagation of the SCC is indeed more complex: the Super Cloud Cluster is composed by a nebulosis of so called “Cloud Clusters” (CC) of a smaller scale (about several hundreds of kilometers) which are moving westward (that's to say in the opposite direction of the global system) pushed by the alizees background winds into

the tropics. The eastward moving is not continuous in time: each cloud cluster has a life expectancy which is about 2 days, and when one disappears, the next one will be

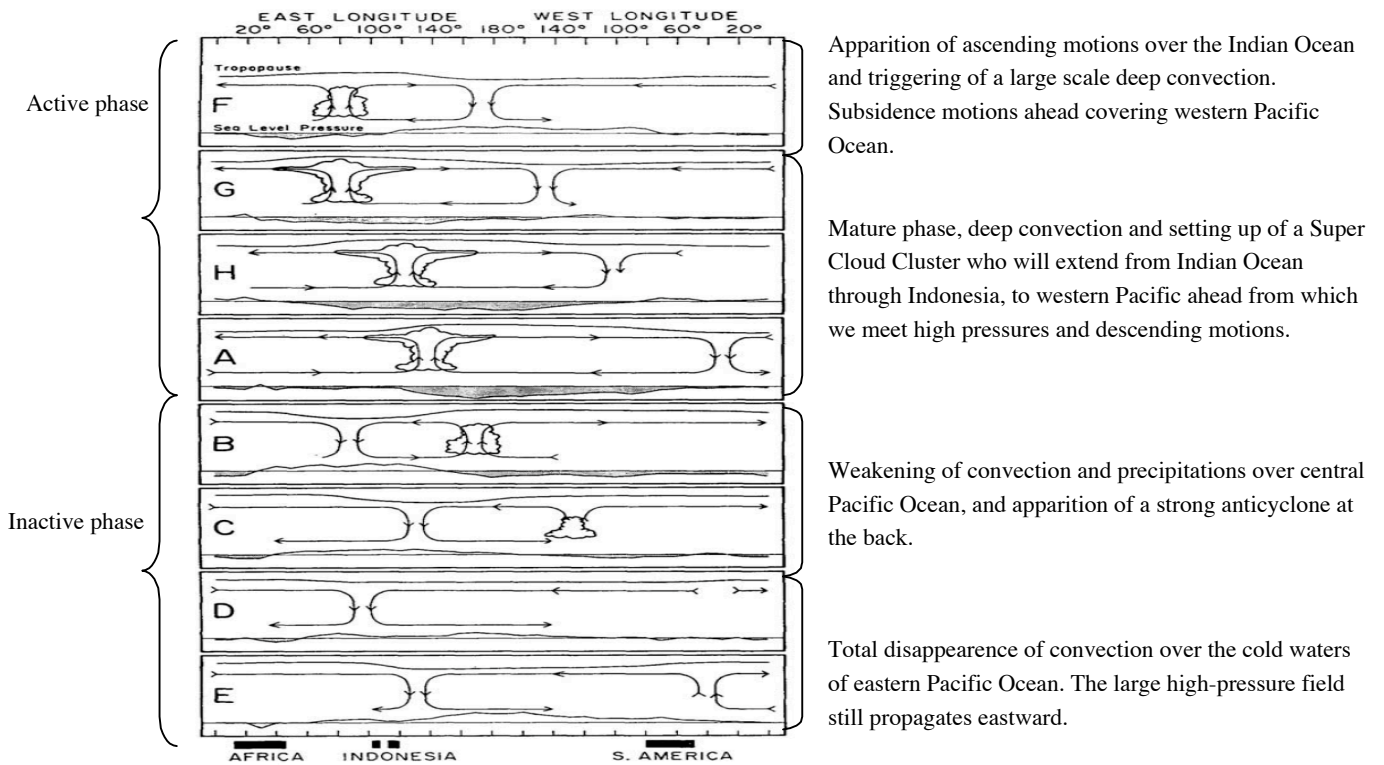


Figure 2 : The different phases of the eastward propagating equatorial MJO wave

Simplified scheme of the equatorial wave in terms of sea level pressure oscillations:

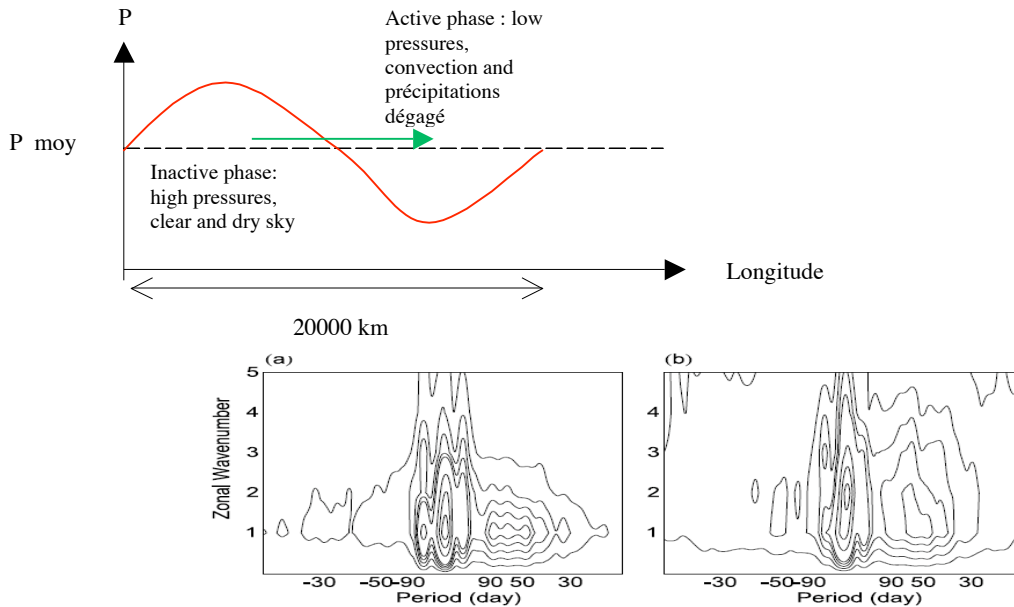


Figure 3 : Wave number-period for the winds at a) 850hpa and b) 200hpa obtained from reanalysis radiosonde data from 1979 to 1998 averaged in a zone [20°S-20°N][60°E:180°E](Zhang, 2005). A wave-nuhsaer equal to 1 means a wave-length of 20000 km, if it is 2, the wave-length is half, and etc.. We can observe an asymmetry favourable to westward waves of whom the most prominent frequency is 50 days, for the surface-winds like for high-troposphere-winds.(Zhang,2005)

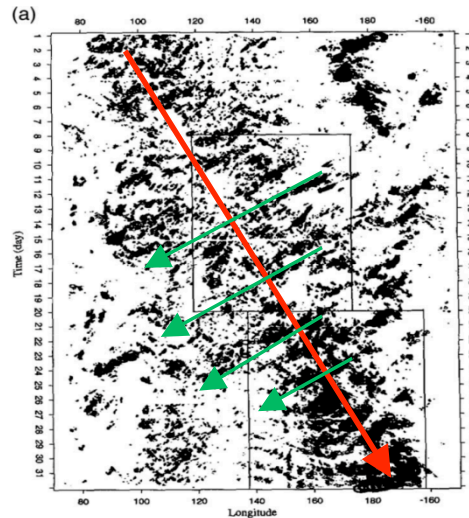


Figure 4 : Same diagram as in fig 1 on which we make appear the mean eastward of the Super Cloud Cluster (red arrow) and also the westward trajectories of the several individual Cloud Clusters (green arrows).

more at the east than the latter. As a result we have on average, eastward motion with speed between 3 to 6 (5 m/s in most of the cases) (see fig.4)

- Occurrence zone :

The active zone of MJO is situated over the so called « Warm-pool », that's to say the area which is extending from the Indian Ocean to the central Pacific Ocean where the Sea Surface Temperature (SST) throughout the year is more than 26°C (even 28°C in the Indonesian archipelago) to a depth of 200 m. Those large volumes of warm water give the principal energy for sustaining tropical convection; that's to say heat and moisture (latent heat). Such high SST helps in maintaining higher rate of evaporation (thus supply moisture for clouds) and vertical instability. Indeed the warm air can contain more water vapour than cold air and is vertically more “unstable” for 3 reasons:

1. Warm air is lighter than cold air
2. Moistened air is lighter than dry air
3. When cooled in clouds, the water vapour condenses and releases more latent heat

$$\text{Evaporation rate} = E = f(u)(e_s - e_a)$$

Where

- e_s = Saturation pressure of the water vapor at SST
- e_a = Relative pressure of water vapor in the ambient air

- $t = SST$
- $f(u) = \text{proportionnal relationship with wind speed}$

While $e_s(t)$ is given by $e_s = 611 * \exp\left(\frac{17,27 * t}{273,3 + t}\right)$ (in Pa units)

This warm and moistened marine air can be in a perpetual state of “conditional instability”, that’s to say in a meta-stable state for which any external perturbation which leads to it’s ascent till the condensation-point altitude (like for example due to a wind convergence, an orographic forcing or a radiative forcing) leads to a deep convection (that’s to say the raise of an air parcel till the top of troposphere by positive buoyancy) and triggers precipitating clouds formation like cumulonimbus. We will develop a little this notion of instability few pages later in this introducing part.

- Seasonal cycle:

2 peaks in the MJO activity are observed in a year:

- The first one during the austral summer, during the north Australian monsoon, between November and February
- The second one, less prominent, during boreal summer between May to August when the south Asian monsoon occurs

That can be explained in great part regarding the seasonal migration of the Inter-Tropical Convergence Zone (ITCZ). The ITCZ is a low pressure zone near the equator rounding the globe corresponding to a “meteorological equator”: that’s to say being a low pressure zone, wind converges and maximum of precipitations occurs. This line is however not continuous in space and time and not properly defined, particularly over east-Africa.

In order to explain more precisely what means the ITCZ, we’ll take the example of a situation of austral spring: the latitude where is the maximum solar flux is situated south from the equator, this maximum will approach the tropic of Capricorn while advancing the season till reaching this latitude at the summer solstice, then it goes again northward. This intense solar

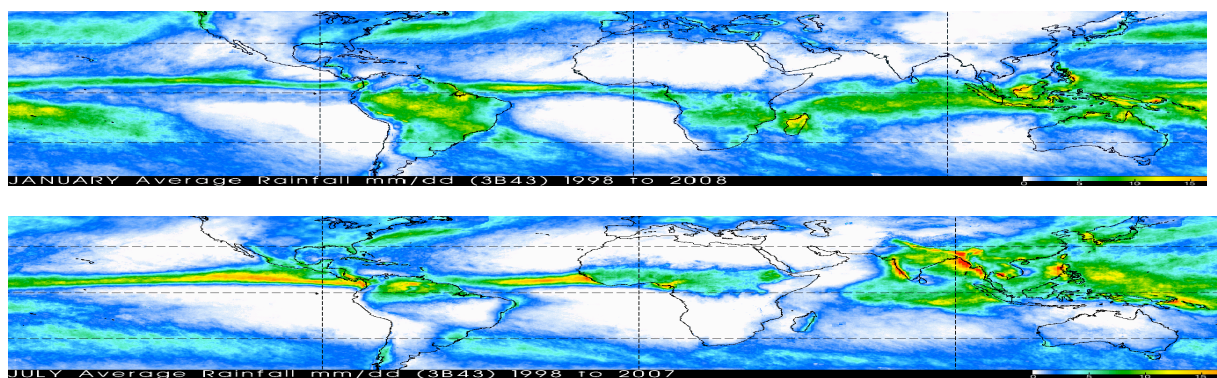


Figure 5 : Daily precipitations averaged over 10 years for the months of January and July thanks to the TRMM satellite (Tropical Rainfall Measurement Mission). It makes appear the extremes meridional situations of the ITCZ for each hemisphere, those two limits corresponds to the maximum of monsoon meridional motions.

radiative forcing over those regions tends to increase SST and thereby the moist static energy of the surface air. This increases conditional instability which only needs low level convergence to trigger large-scale ascending motions. The resulting heat release in the clouds makes the upper atmosphere warmer, that results in a low pressure belt near by a thousand kilometres width which in term maintains plenty of storm clouds all around the globe: this is the so called ITCZ (see [fig.5](#)).

Important remark:

The ITCZ is not merged with the latitude of maximum solar forcing even if their motions are more or less in phase.

The MJO activity is strongly dependent on the seasonal oscillations of the ITCZ around the equator, it's triggering over the Indian Ocean is synchronized with the arrival of the ITCZ in that zone.

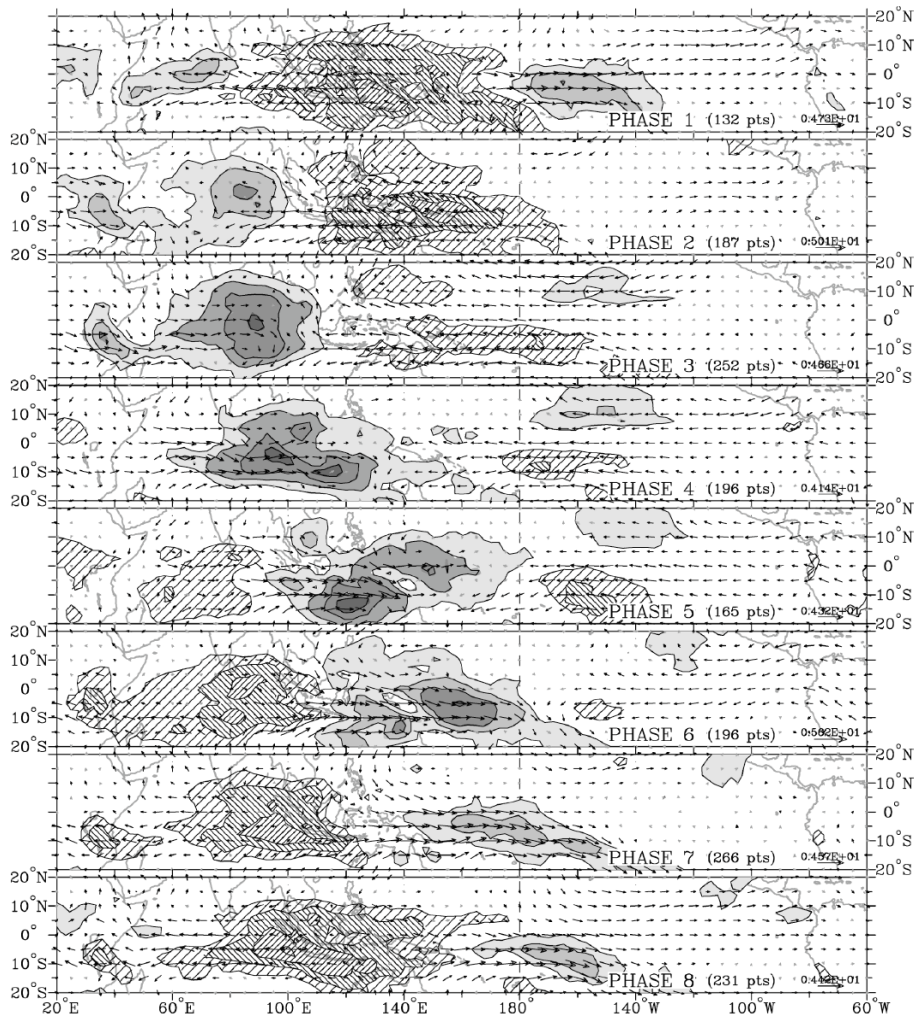
1.3. Visualisation methods of MJO:

In order to display MJO, we usually use:

- 2 atmospheric variables: **wind vectors at 850 and 200hpa** measured from reanalysed radiosonde data. Those ones inform us about convergence and divergence zones on the top and in the low troposphere, thus allowing the climatologists to track depressions and anticyclones.
- 1 top of the atmosphere variable: **Outgoing Long wave Radiation (OLR)** emitted by the Earth measured by the satellites. When deep clouds are present, effective emission corresponds to their top and OLR values are less. Thus OLR can give us the extent of deep cloud cover. More OLR are detected, less is the total cloud cover, and thus, higher are the ground temperatures.

The most rigorous method for extracting this atmospheric wave was realised by a study of anomalies fields for the variables described before; a wave can only be detected by the variations of the properties it produces over the crossed region. What is interesting here is thus to quantify the variability of winds and OLR by the analysis of their anomalies.

While it is easier to detect an MJO from satellite cloud pictures (e.g fig 1), quantifying it has proved to be more difficult. Two climatologists by the name of Wheeler and Hendon from the BMRC (Bureau of Meteorology Research Centre, in Melbourne) proposed in an article published in February 2004 titled as "An all-season real time multivariate MJO index" in the Monthly Weather Review a filtering method for detecting the MJO by the mean of empirical orthogonal functions (EOF). They used daily data of OLR, 850 and 200hpa winds, from 1979 to 2001 between the 15°S and 15°N latitudes that they projected in the vector space of which the base is formed by the eigen-vectors of the covariance matrix of each variable. Hence they could draw maps (one for each time-step) indicating the real time anomaly for each variable. After removal of the weakest variances, relative to other types of atmospheric waves than we are interested in, they could precisely extract the MJO signal, as it is displayed in [fig 6](#).



Inactive phase

Active phase: we clearly notice the precipitation motion displayed by negative OLR anomalies, strong westerlies behind the SCC and easterlies ahead from it. The lowest pressures are at the meeting point of those fluxes.

Inactive phase: the important positive anomalies consecutive to the SCC testifies a strong solar heating, we can observe mainly easterly winds. A strong anticyclone is standing over that region.

Figure 6 : The different phases of MJO extracted by EOF analysis, here displayed by mean anomalies of 850hpa winds and OLR for the 1979-2001 period. The hatched zones correspond to, respectively from the most central to the most remote, positive OLR anomalies of more than 22.5 ; 15 ; 7.5 W/m₂. The filled grey zones correspond to the opposite anomalies. The black arrows represents the positive wind-speed anomalies, their value of the greatest anomaly is displayed in the right back corner of each map.

This study also depicted the large scale vertical structure of MJO.

(See fig.7).

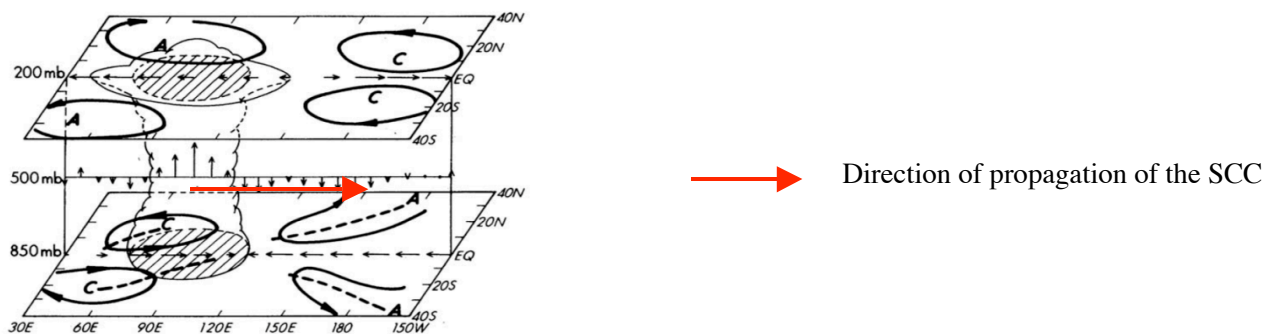


Figure 7 : Scheme of the large scale MJO's vertical structure. The SCC is situated at the meeting point of two depressions situated from part and other of the equator which push it eastward and which maintain strong ascending motions.

1.3. A brief description of the tropical climatology and atmospheric general circulation:

The sun remains the main energy source for the atmospheric heat engine (geothermic energy has a negligible contribution), but only inter-tropical regions have a positive net radiative balance (i.e incoming from sun is more than that lost due to emission). In addition the meridional redistribution of energy is only realised by the two fluids namely water and air. We won't speak about the ocean circulation here. Concerning the atmosphere, the thermal phenomena responsible for carrying heat from the equator to the pole is convection: knowing that the air has a very low thermal conductivity, the contribution of conduction is negligible. The solar heating of the atmosphere is at its maximum at the lowest layers of the atmosphere because of its proximity to ground which is hotter than the air during the day (atmosphere is a poor absorber of solar radiation and most of the solar energy is absorbed by the surface). Solar heating helps in the initial ascent (dry convection) but condensation is needed to take air parcels to the tropopause level by maintaining positive buoyancy (results in deep convection). This moist adiabatic ascent process takes typically 1 hour and water vapour is removed from the air at the cold temperatures of the upper troposphere. From those large scale ascent motions are set up depressions. The air coming out from the deep cloud systems, by radiative cooling slowly subsides (moves down) and it takes around 25 days to return to the surface. The subsidence regions produce anticyclones. As a result, we have a quasi-permanent low pressure belt over the equatorial belt and a strong anticyclone around the 30°S and 30°N latitudes generating the westward alizees-winds: this is the so called Hadley cell. From this disequilibrium are triggered winds which will ensure the horizontal transport of heat, by a permanent mix of antagonist air-masses. Finally we can say that this is in the lowest latitudes, always in energy excess, where the general circulation takes its source.

That's one of the reasons for the current interest in tropical climatology; from the variability of atmospheric an oceanic inter-tropical phenomenon are depending other events in the mid and high latitudes.

We could give as an example the oceanic phenomena usually called "El Nino" in the Pacific Ocean (as a reference to the birth of Jesus Christ, knowing that it starts most of the time during the Christmas period); that's to say the abnormal motion of large volumes of warm water from Indonesia to Peruvian coasts. This sudden variation in the distribution of SST enhances several phenomena all over the globe, even further beyond the tropics (see [fig 8](#)).

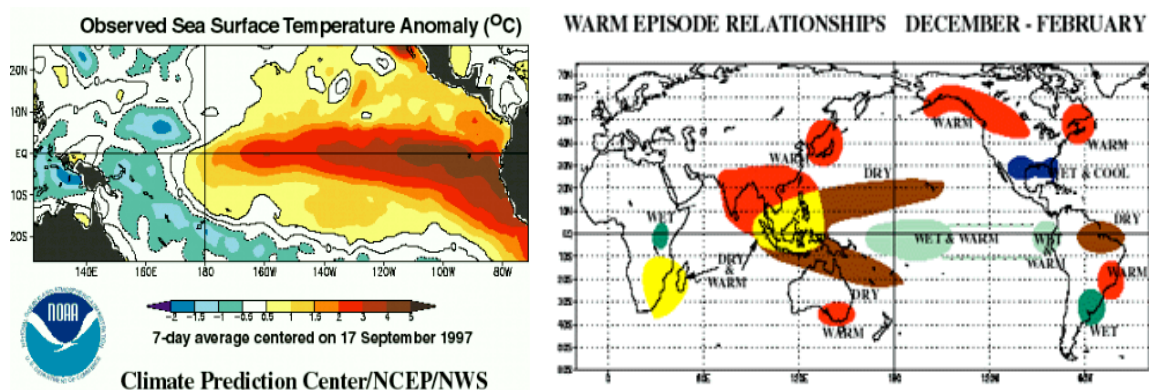


Figure 8 : SST anomalies during an ENSO event (left window) and its global effects (right window)

It looks clear that the accuracy of the Atmospheric General Circulation Models (AGCM), depends on a great part of our understanding of climate within the tropics.

The MJOs take definitive part into those global-scale processes. While its structure and kinematics are now well described, its dynamics remains to be fully explained by theory.

1.4. Main purposes of the project:

- The first goal is to find a different way of tracking the MJO, knowing that the typical proxies used in the previous studies of this phenomenon were OLR and 850hpa winds. Actually those two proxies are very useful to describe MJO's kinematic but they don't really give us information about vertical structure and space-time energy variations generated by MJOs. For this we will use the variable **Moist static energy** $h = C_p * T + L_v * q + g * z$ (kJ/kg) where L_v is the latent heat of evaporation of water (kJ/kg), q is the specific humidity (kg/kg), z is height (m), g is acceleration due to the gravity (m/s²).
- The second purpose is to define a favourable background for the eastward propagation of the MJO, in this part we will show that without a surface westerly wind background over the equatorial Indian Ocean, the chances to have an MJO is very less.
- Finally we will look at an eventual correlation between moist static energy oscillations over equatorial Africa, Indian Ocean and Indonesia in order to find the place where the wave could be set up. Such a correlation could be very interesting because equatorial Africa is not recognized as being crossed by the MJO (which born about over the 70th longitude east), hence it could open a new hypothesis about the real place where the MJO is set up. This statistical analysis based on FFT transform (on Matlab) will be done by comparing the behaviour in time of moist static energy at 500hpa averaged over each of the three regions described as below. We will compare the results for 9 strong MJO events and 9 weak MJO events and try to find the differences between, if differences are there.

2. Data and methodology

This study is based on reanalyses data freely available on the ECMWF (European Centre for Medium-Range Weather Forecast) proxy server. Over the past decade, reanalyses of multi-decadal series of past observations have become an important and widely utilized resource for the study of atmospheric and oceanic processes and predictability. Reanalysis products are used increasingly in many fields that require an observational record of the state of either the atmosphere or its underlying land and ocean surfaces. Reanalyses data are obtained by interpolation in space and time of daily radiosonde and in-situ data optimised using governing equations.

These reanalysis data have been recognized as a powerful tool for diagnosing the climate variations in the tropics, thus we can consider them as being reliable.

In this study, we used 'ERA 40' data from 1957 till 2001, which is the most recent reanalysis product freely available from ECMWF, combining in situ observations and satellites products.

The database is time-series of two kinds of variables:

1. **Atmospheric variables:** such as

- Winds $U, V(m/s)$
- Temperature $T(K)$
- Specific humidity $q(kg/kg)$
- Geo-potential height $Z(m^2/s^2)$ where $Z=g*z$ and z is altitude

2. **Surface variables:** such as

- Winds $U, V(m/s)$

The time series used in this study are taken within the period 1957- 2001 and the time-unit is the day. Basically we have taken one sample per day corresponding to that at 12h00 GMT for all these variables.

2.1. Time-longitude-filled diagrams and maps on Ferret:

The time-space diagrams and maps were drawn with software called FERRET, which can only be used on a Linux machine. This software developed in the NOAA institute (Miami) is an equivalent of GRADS which is the reference for the atmospheric sciences, but FERRET has the advantage to compute also oceanographic data, that's why its use is more and more spread into the climatologists' community.

- The maps are simply built by taking a meantime, for each latitude/longitude point, of one variable at a particular level of the atmosphere (or at the surface).
- The time-longitude-filled (Hovmoller) diagrams are built by taking the **space average within the latitudes 15S and 15N of h** at a particular level (200hpa or 500hpa).

2.2. FFT transforms and wavelet analysis on Matlab for comparing moist static energy h (at 500hpa) activity over Africa, central Indian Ocean and Indonesian archipelago

2.3.1. The space selection:

In order to display a possible relation of frequencies for moist static energy at 500hpa between equatorial Africa, central Indian Ocean and Indonesian archipelago (fig 9) during strong MJO events we first define three boxes within the tropics where we have followed in time the space-average (in each box) of moist static energy (h).

- The first box is ($[10^{\circ}\text{E}:30^{\circ}\text{E}];[15^{\circ}\text{S}:15^{\circ}\text{N}]$) over Africa
- The second one is ($[80^{\circ}\text{E}:100^{\circ}\text{E}][15^{\circ}\text{S}:15^{\circ}\text{N}]$) over Indian Ocean
- The last one is ($[130^{\circ}\text{E}:150^{\circ}\text{E}][15^{\circ}\text{S}:15^{\circ}\text{N}]$) over New Guinea

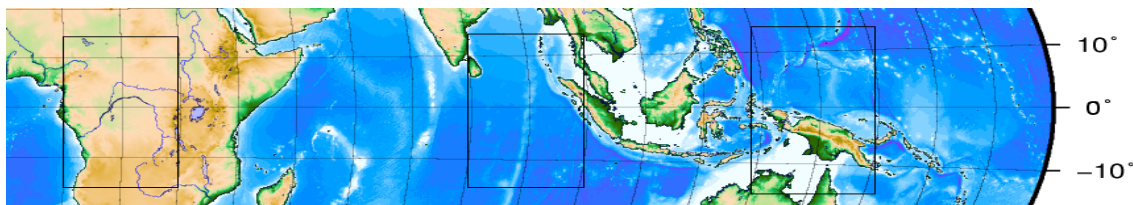


Figure 9: The three boxes chosen for the wavelet analysis of h at 500hpa

These three boxes were chosen after comparing many longitude-time diagrams, and are likely to be the best spatial samples able to track the MJO crossing: indeed the two last boxes are corresponding to the peak of activity of MJO on average, and the first one is likely to be the most correlated with the latter, regarding MJO by the mean of h (500hpa).

If we had taken larger boxes, the average of h (500hpa) might have no meaning.

2.3.2. The time selection:

In order to understand in the behaviour of h between active and weak MJO periods, we like to compare its time series representative of these two periods. In the article by Wheeler and Hendon evoked below “An all-season multivariate MJO index”, we can find a plot of real-time variance of OLR, which is the best proxy for MJO, within the 1974- 2003 period. It gives us a real-time quantification of MJO intensity, thus a good reference for sorting strong and weak MJO in the comparative study we’ll describe later (fig 10).

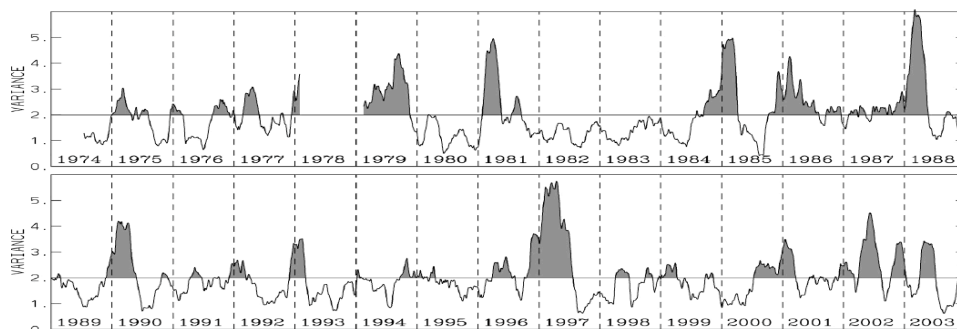


Figure 10: Time series of a 91-day running mean $\text{RMM1}+\text{RMM2}$ (principal components of the EOF) showing the low-frequency modulation of the variance of the signal of the MJO: shaded times are MJO active period

In the above plot, all the periods of time which correspond to a real-time OLR variance over 2 are considered as strong MJO events, and inversely less than 2 considered as weak MJO.

For this statistical analysis we compare nine strong MJO events with nine weak MJO events, each time series forming a couple (Strong MJO/Weak MJO) will get the same length as its antagonist, and finally we will get nine of those couples ([Table 1](#)). For each time series (18*3 (boxes) = 54 total), we extracted the peaks of the h (500hpa) periodogram obtained after FFT transform and normalization by the red noise.

Case	Strong MJO	Weak MJO
1	01/05/1979-31/12/1979 +MJO79	01/03/1982-30/10/1982 -MJO82
2	01/12/1980-31/05/1981 +MJO80-81	01/11/1982-30/04/1983 -MJO82-83
3	01/09/1984-31/03/1985 +MJO84-85	01/07/1988-31/12/1988 -MJO88
4	01/10/1985-31/05/1986 +MJO85-86	01/01/1991-31/08/1992 -MJO91-92
5	01/11/1987-31/05/1988 +MJO87-88	01/05/1993-30/11/1993 -MJO93
6	01/10/1989-30/06/1990 +MJO89-90	01/02/1980-30/10/1980 -MJO80
7	01/10/1992-30/04/1993 +MJO92-93	01/05/1994-31/12/1994 -MJO94
8	01/11/1996-30/06/1997 +MJO96-97	01/09/1997-30/04/1998 -MJO97-98(or ENSO97-98)
9	01/06/2000-31/01/2001 +MJO00-01	01/12/1999-31/07/2000 -MJO99-00

Table 1: The nine couple of time series selected thanks to the MJO index

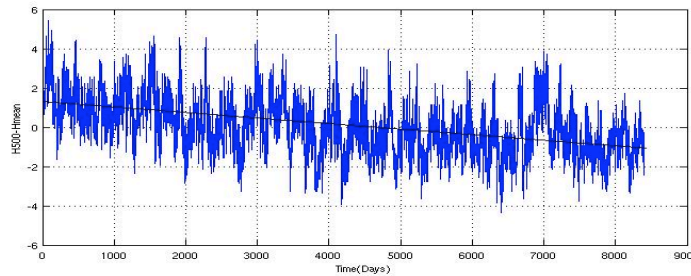
We will describe now all the filtering steps needed for each box before getting the adapted periodograms which will be interpreted in the third part (Results and Discussion).

a) Removal of the mean:

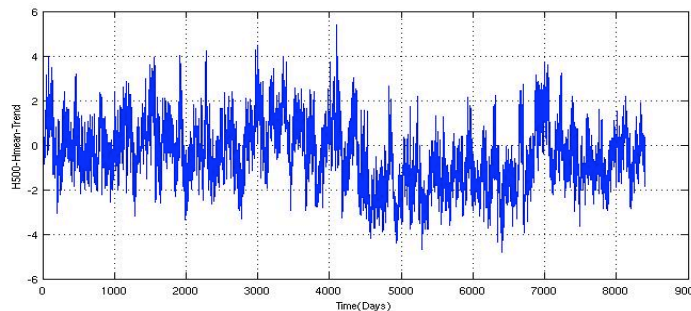
For each of the three boxes, we first have a large time series of h (500hpa) over 23 years from 1979 to 2001 included (8401 days) which corresponds to the total period of time we study, so the first step consists in the removal of the mean, in order to get directly the h (500hpa) anomaly which is more concrete than absolute values in our study. Let's take the African box for example:

b) Removal of the linear trend (also called infinite trend) :

At this time we get a plot like it with an linear trend for Africa:

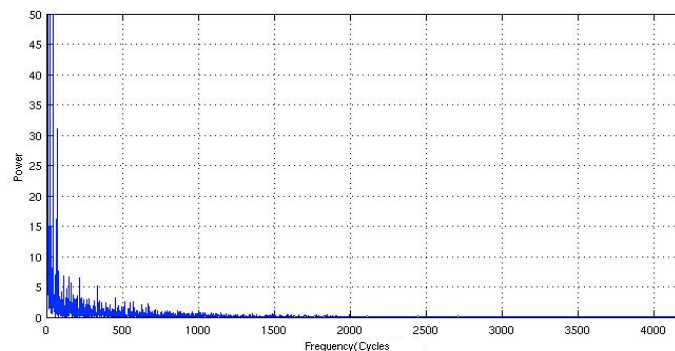


This infinite trend has to be removed because it will cause a parasite signal in the FFT transform, if we don't do that we will observe a very strong spectral peak at very low frequencies. For this we just subtract the present signal by the best fit linear trend, like for the mean and we obtain the signal shown below:



c) Red noise:

If we do right now the FFT transform of that signal, we will get these frequency power spectra (after division by N_ where N is the length of the time series, here it is 8401) for Africa:



Here we can easily see that there is a rising baseline for the lowest frequencies: that is called the Red noise, that's to say the increase of the real part of the Fourier coefficients at low

frequencies. Indeed, by working with large time series (like in climatology) the FFT transform favours low frequencies, and those low frequencies introduce a noise in the frequency-power spectra that we have to remove by dividing it by the red noise spectra: this is called the normalisation by red noise.

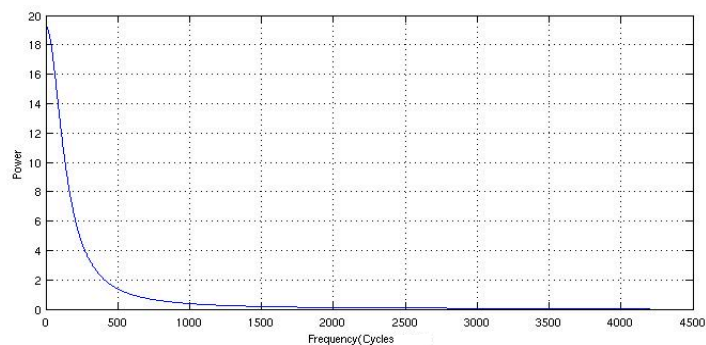
The red noise spectrum is given by the following formula (Torrence and Compo 1998, “A practical guide to wavelet analysis”):

$$P_k = \frac{1 - \alpha^2}{1 + \alpha^2 - 2\alpha \cos(2\pi k/N)},$$

Where

- P_k is the power at frequency k
- α is lag-1 autocorrelation coefficient of the time series
- k is the frequency index in total cycles in the time series
- N is the length of the time series

Then global red noise calculated using the 23 years data is shown below:

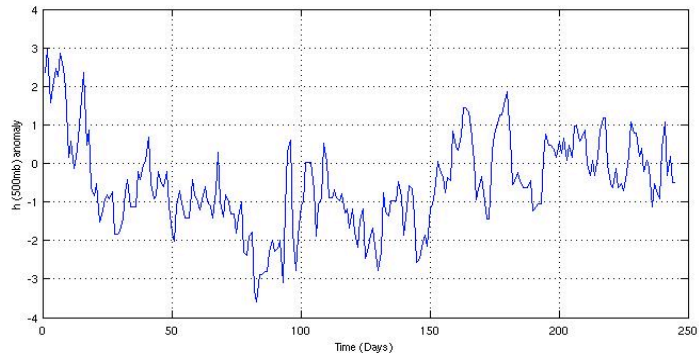


This operation had to be done for the 23 years times series of the three boxes, that's to say Africa, Indian Ocean and Indonesia; hence we obtained the global Red noise spectra for each one of them, corresponding to the 1979-2001 period in which were selected all the couples of Strong/Weak MJO.

d) Selection of the 54 time series and altering of the 30 initial and end days fluctuations by cosine tapering:

At this step, within each of the three 23 years time series of h (500 hpa) obtained after removal of mean and trend, we selected for each region (or box) all the interesting 18 time series of strong and weak MJO (9 strong and 9 weak) according to the periods of time displayed in table 1.

Let's display for example this time series of h (500) anomaly for Africa in a strong MJO period (01/05/79-31/12/79):

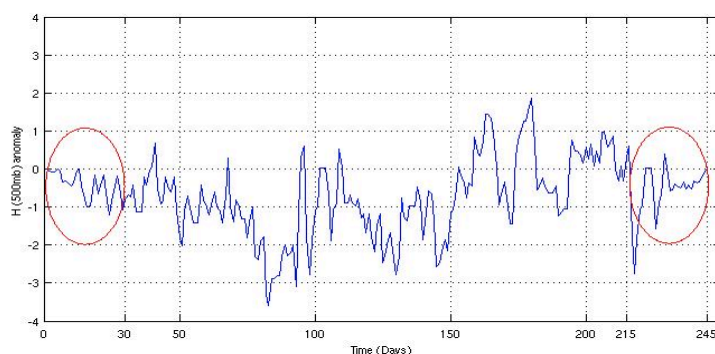


By doing an FFT transform, we only want to catch periods or frequencies in the time series. However, when a time series is selected, end points are not zero and taking FFT of such time series can result in spurious frequencies. To minimize this effect, a cosine smothering is applied to the end points. Indeed, we have to focus the FFT only in the central parts of the time series, because the initial and the end fluctuations do not have a complete period, that causes parasites in the frequency-power spectra. This filtering method is called the cosine tapering.

For this we multiply:

- The firsts 30 values by $\cos\left(\frac{\pi}{2} * \frac{t_0 + \tau - t}{\tau}\right)$ where $\tau = 30$ days
- The lasts 30 values by $\cos\left(\frac{\pi}{2} * \frac{t + \tau - t_f}{\tau}\right)$

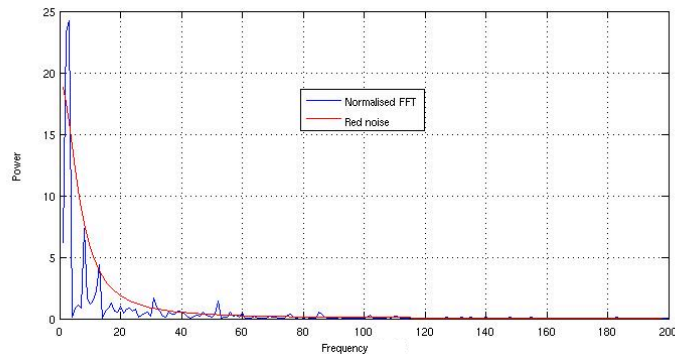
Then we obtain the following time series. Note that the major portion of the signal remains unaffected and end points approach zero value smoothly.



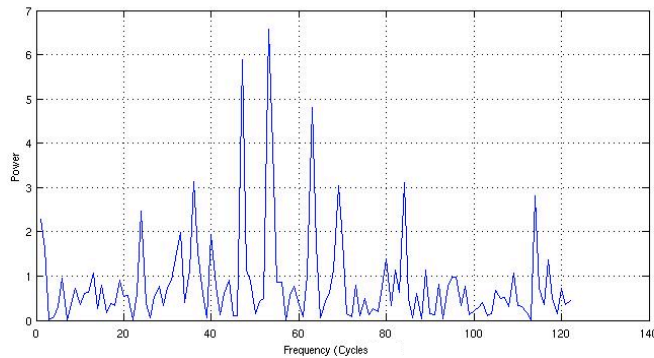
e) Normalisation by the global red noise:

Normally the background is assumed to have a red noise. This could be a white noise (all frequencies have equal power) or frequency dependent power (e.g red noise). Weather signals tend to have red noise. Hence we normalize the actual spectra by the corresponding red noise.

Last thing to do now is to divide this normalise spectra by the global Red-noise in order to get the final spectra, then from this spectra:



We get this final one:



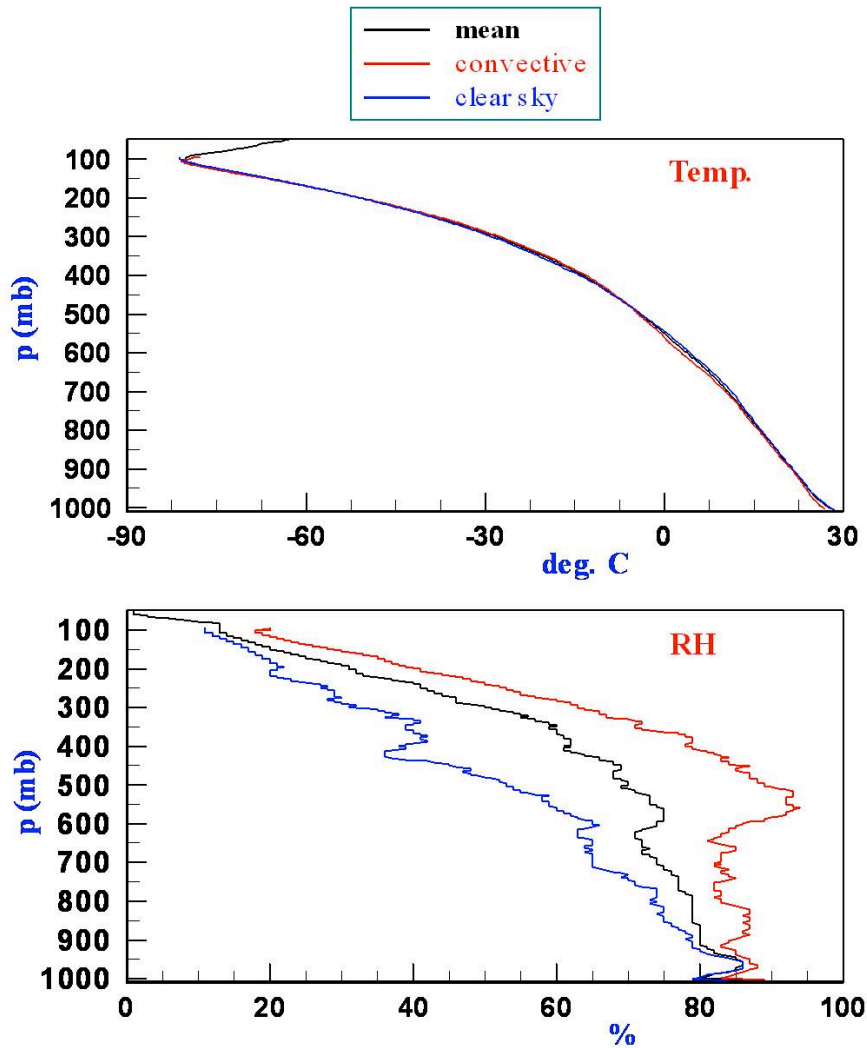
Statistical test are applied to know the significance of the resulating signal. It is found that when normalized spectral value exceeds 1.25, then the signal is significant at 95% confidence level (Wheeler and Hendon 2008). That is to say there is a 95% chance that the spectral peak observed is due to a real signal in the time series and only 5% chance that is due to noise.

f) Why choosing the moist static energy at 500hpa?

Moist static energy is a the total energy contained in a unit mass of air in the atmosphere in terms of latent heat, potential energy and sensible heat (kinetic energy is too small in comparison and normally neglected).

The moist static energy at 500hpa is actually a good proxy for deep convection because shallow convection processes can only reach 850 to 800hpa in altitude (responsible for the formation of cumulus clouds in most of the cases). Hence a high most static energy anomaly at 500hpa is mostly related with a high specific humidity anomaly at this level, that's to say a strong ascending motion which leads humidity in the mid and high levels of the atmosphere (and therefore latent heat).

The [fig 11](#) shows the averaged vertical profiles of Rh (relative humidity) and temperature T during deep convection events and non-convective events.



Vertical profiles during BOBMEX.

Figure 11 : Mean vertical profiles of temperatures (upper window) and relative humidity (lower window) during convective events (red) and stable atmosphere (blue) during BOBMEX ship measurements (Bay Of Bengal Monsoon EXperiment)

We can see that, at 500hpa, the most prominent difference between both cases is for $\Delta Rh (=Rh(red)-Rh(blue))$, at that level temperatures are quasi equal, then $\Delta T (=T(red)-T(blue))$ can be supposed negligible (however ΔT is more important at the surface or at 600hpa where we can have $\Delta T=2^{\circ}C$ even if it's not obvious in that plot because of a problem of scale). Knowing that Rh is a function of T and q, we can deduce that this high ΔRh is mostly due to a high Δq , regarding the negligible ΔT .

Hence the h (500hpa) oscillations we observe during MJO events are mostly meaning oscillations in q at that level: this is an important point on the basis of which we will develop an important hypothesis in the concluding part.

3. Results and discussion

3.1. MJO tracking by moist static energy at 500hpa:

First let's look at the longitude-time-filled diagram of h (500hpa) for two strong MJO events (Hovmoller diagram [fig 12](#)).

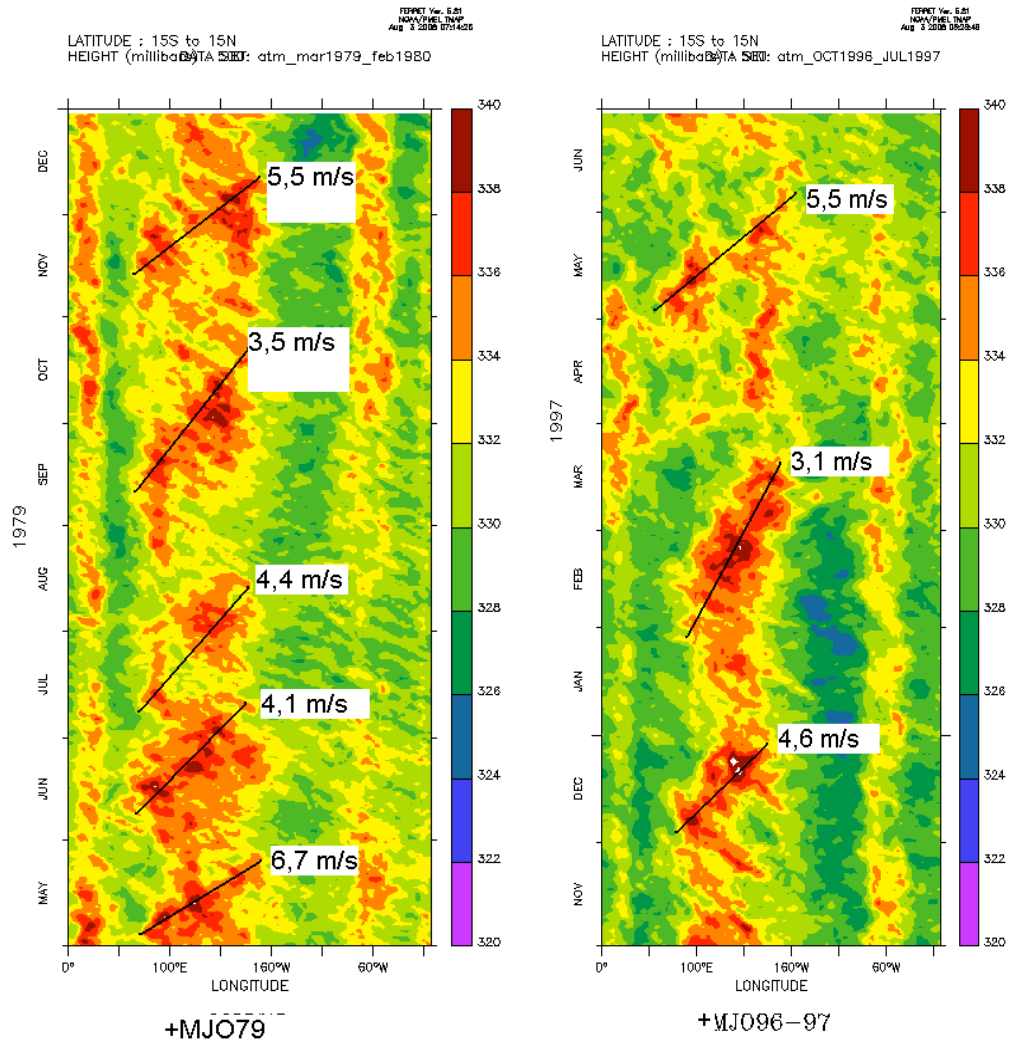


Figure 12: Longitude-time diagrams for h (500hpa) averaged between 15°S-15°-N for two strong MJO (refer to table 1)

We can see in this figure a prominent eastward moving of high h (500hpa) from central Indian Ocean through Indonesia till central Pacific Ocean during strong MJO events, this zone is exactly corresponding to the typical propagation zone of the MJO regarding the minimum of OLR (typically observed in most of the previous studies dealing with the MJO).

Moreover the average propagation speed of h corresponds to that of the MJO one's which is around 5 m/s. Thus we can consider that this h proxy can be adapted to the tracking of MJOs.

This statement can also be observed for the others strong MJO we have.

3.2. The low level westerly-winds background:

Within the tropics are typically dominating the alizees-winds, which are regular anticyclonic easterlies triggered around the strong anticyclones standing over the 30°S and 30°N latitudes, especially over the oceans as we can see on [fig 13](#). But the only one exception concerns the equatorial Indian Ocean, where in summer as in winter, we have westerly winds on average. This is actually the only one marine region where the 850hpa-wind-profile is inverted.

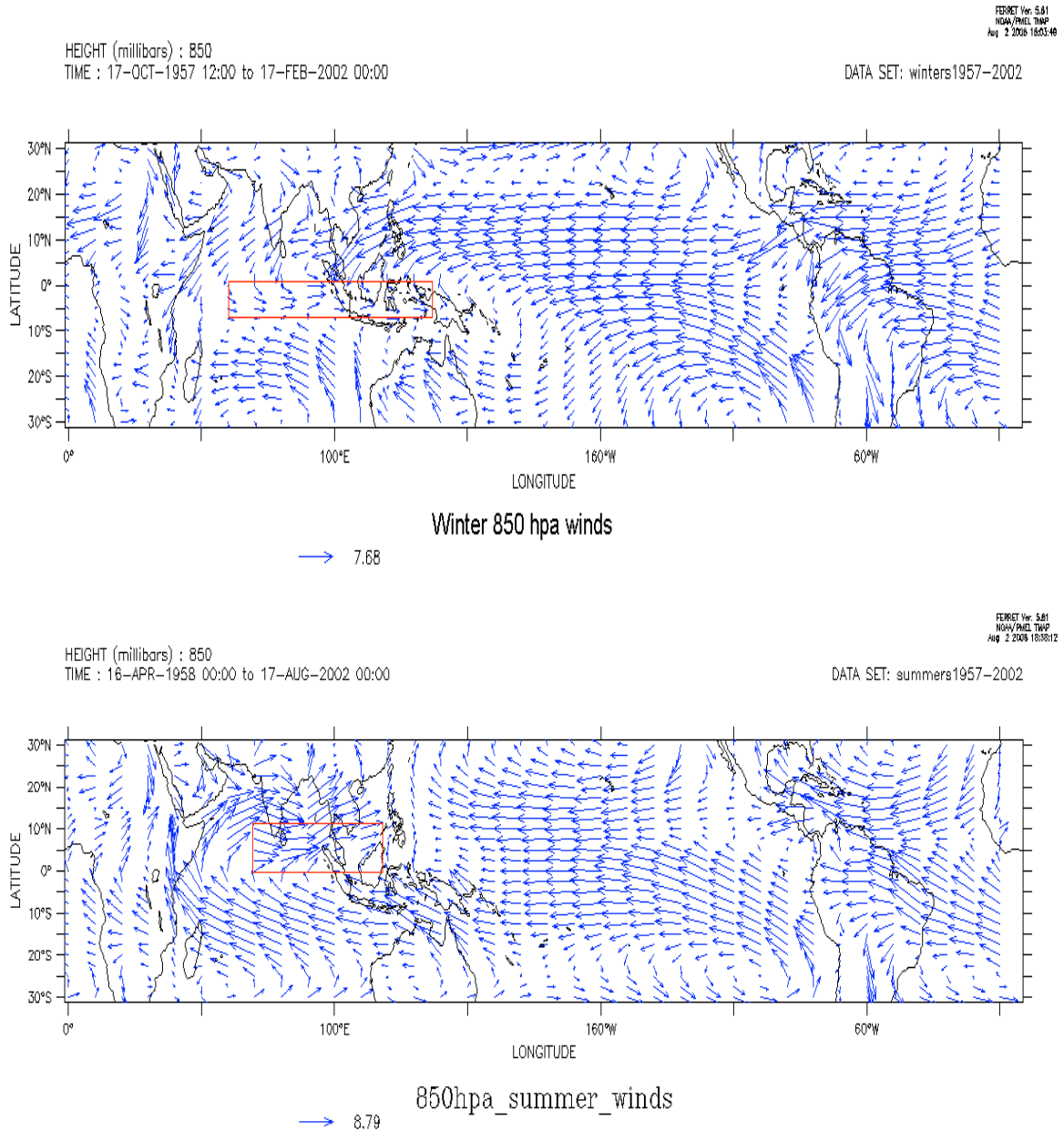


Figure 13 : Zonal-850hpa -winds mean for the months of Novehpaer to February (upper window) and for the months of May to August (lower window) averaged from 1957 to 2002

This background of westerly winds can be favourable to the eastward propagation of an equatorial wave like the MJO. Moreover, the concerned regions where are those westerly

surface winds are strongly corresponding to those which are crossed by the observed MJO. Hence we can suspect this background to help moisture transport through the Indian Ocean and to lead an eastward moving convective instability in that direction also. Actually if we overlay those surface winds onto the average map of moist static energy at **200hpa** (which is also a good proxy for deep convection) like in the [fig 14](#), we can see that during the austral summer, a strong deep convection zone is centred over northern Australia, inversely over the northern part of the Indian subcontinent while boreal summer. Deep convection events are strongly related with low pressures and wind convergence, hence we can guess that those regions, thanks to the pressure gradient combined with the Coriolis force, lead all over the year geostrophic winds from the west over Indian Ocean: indeed, geostrophic winds are turning around low pressures in a trigonometric motion in the North hemisphere and inversely in the South hemisphere.

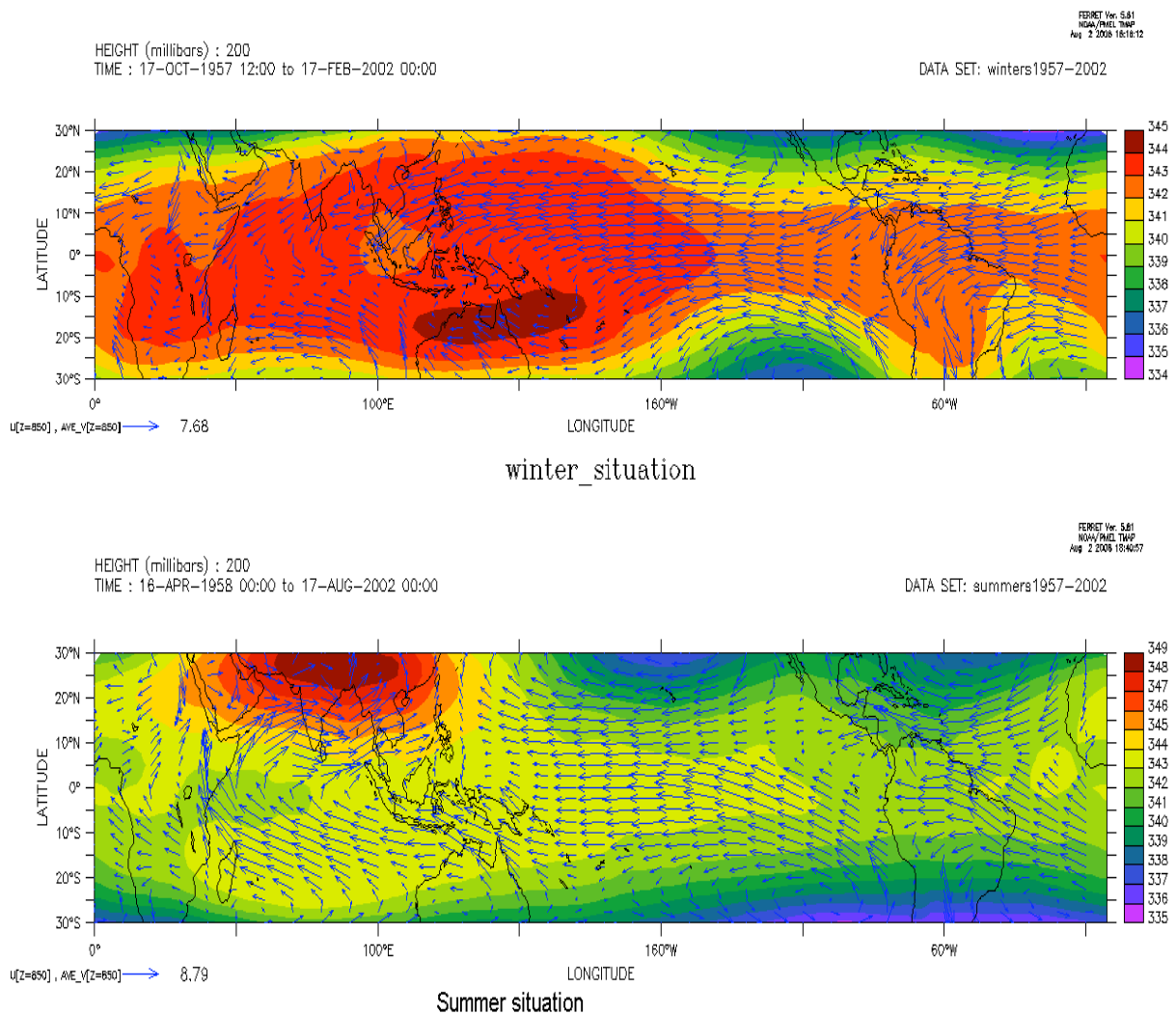


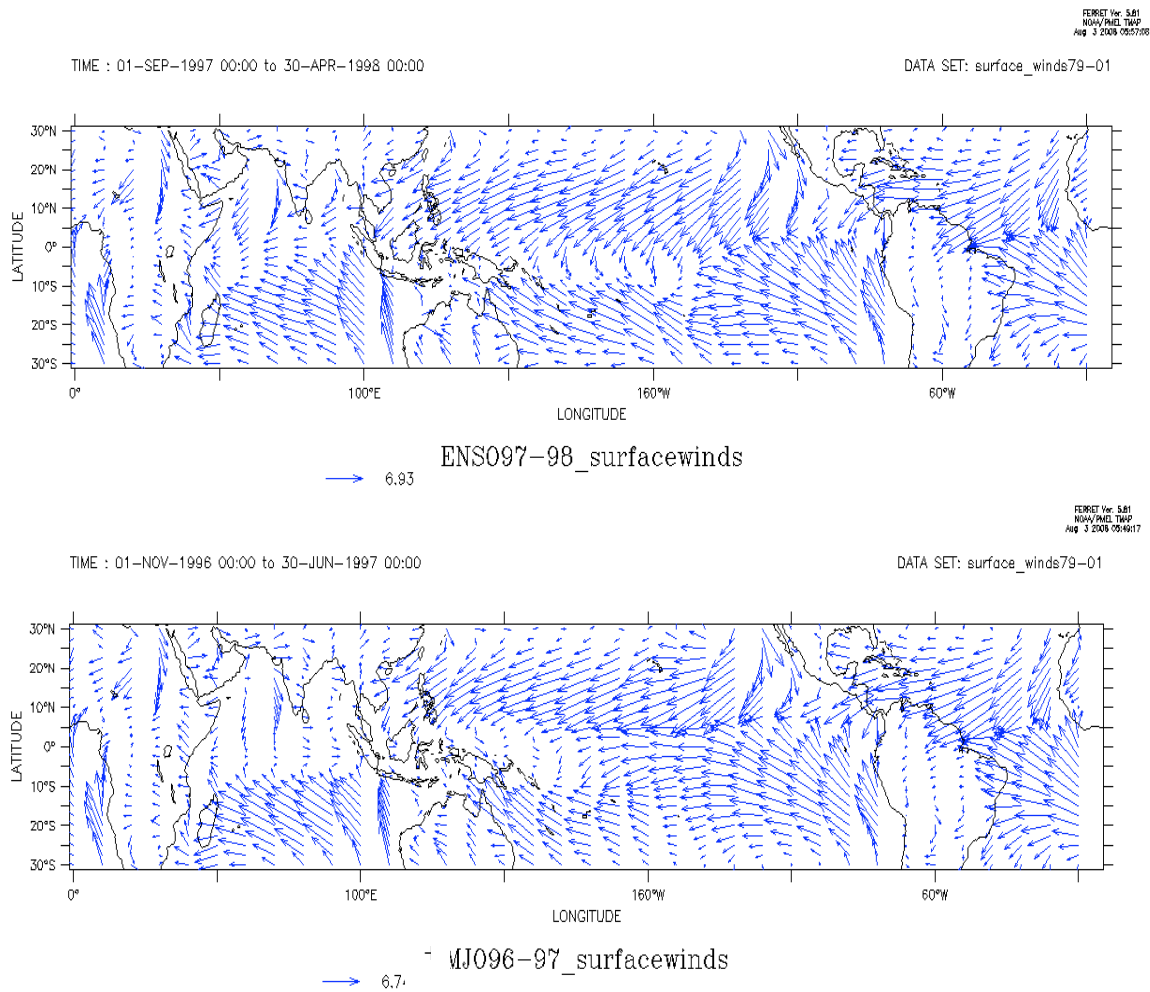
Figure 14 : Zonal-850hpa-winds and h (200hpa) mean for the months of November to February (upper window) and for the months of May to August (lower window) averaged from 1957 to 2002

Those permanent westerly winds over Indian Ocean and easterly winds (alizées) over western Pacific are maintained all over the year a large scale wind convergence over the Indonesian archipelago which actually enhance deep convection in that region and high

precipitations: this zone corresponds to the spatial peak of activity of the MJO where are observed the deepest clouds and the strongest westerly wind anomalies at 850hpa altitude (Zhang 2005, MJO Oscillations).

Thus we can assess that the seasonal fluctuations of the maximum of convection within the 30°S-30°N is the cause of these westerly wind background which possibly leads the MJO during boreal and austral summers, which are the two peak season for MJO activity.

Fig 15 shows the zonal-surface-wind map averaged during an El Nino event (ENSO) (upper window) and a strong MJO event (second window beneath) and the time-longitude of h (500hpa) corresponding to each of them. There we can directly notice during the ENSO event the inversion of surface-wind direction over Indian Ocean, the background of westerlies disappears for easterlies, and we neither can see any periodicity in the signal of moist static energy over Indian Ocean, nor westward moving organised convective system: the MJO signal is thus totally inhibited. On the contrary during a strong MJO event, we can observe the westerlies background on the wind-map and the periodicity of MJO in the time-longitude diagram.



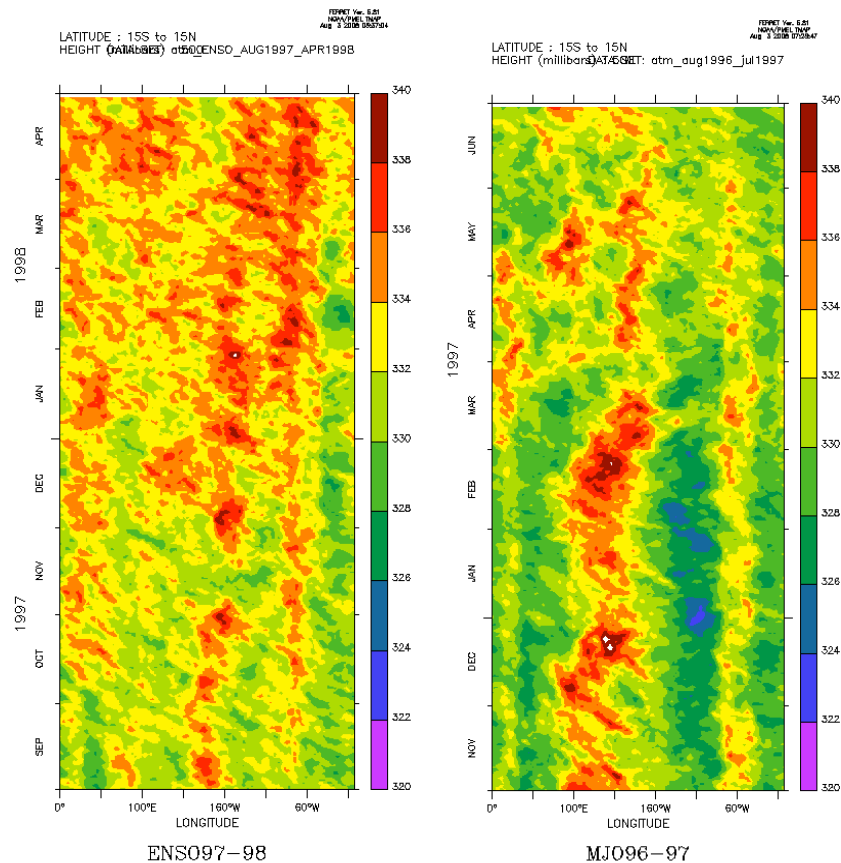
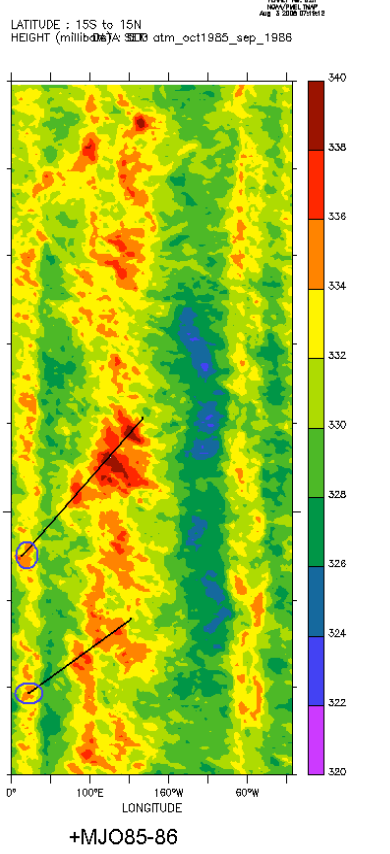
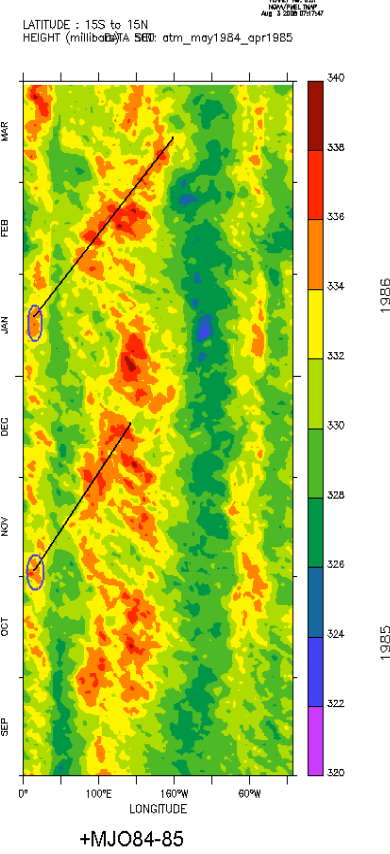
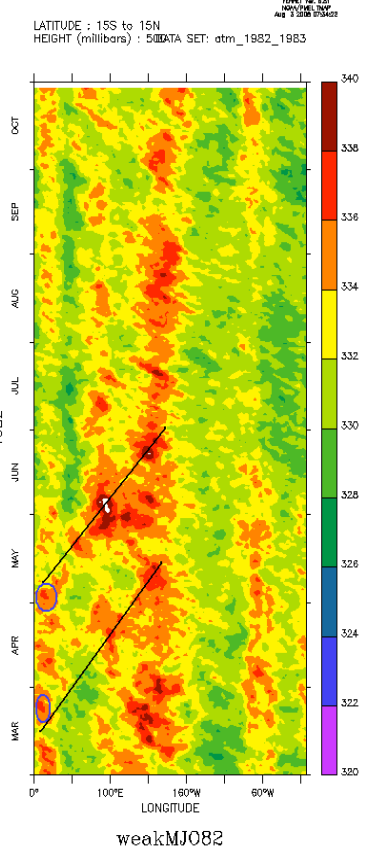
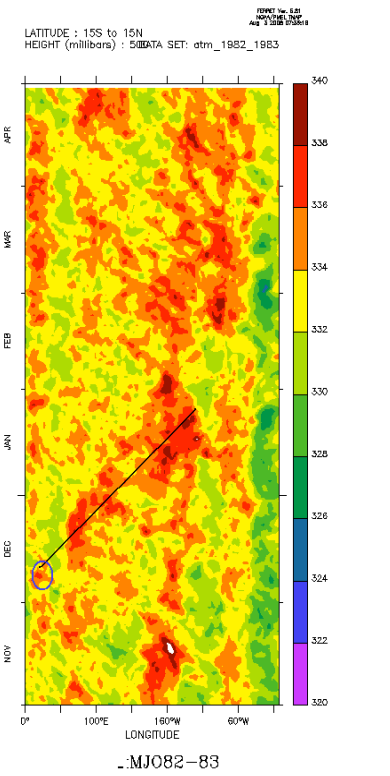
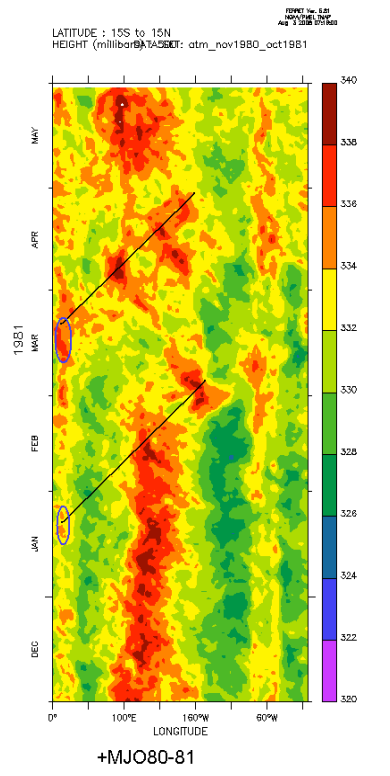
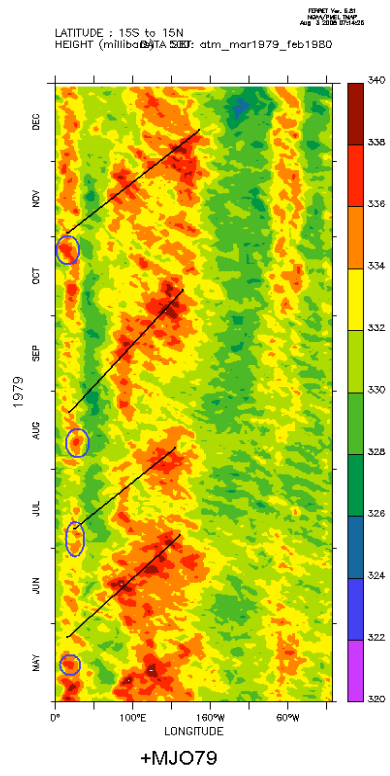


Figure 15: Surface winds and time-longitude diagrams of $h(500\text{ hPa})$ averaged between 15°S-15°N for a weak and strong MJO

A low level westerly winds background over equatorial Indian Ocean seems to be thus a critical condition for the triggering and propagation of the MJO equatorial wave without whom the chances to have an MJO signal are very few.

3.3. A possible correlation between $h(500\text{hpa})$ periodicity over equatorial Africa and $h(500\text{hpa})$ over Indian Ocean and Asia

As we said previously the equatorial Africa is not supposed to be crossed by the MJO inferred from the observations of OLR and 850hpa winds, but the observation of $h(500\text{hpa})$ fluctuations over the central Africa showed in some cases a strong correlation with the MJO's activity over the other concerned regions (Indian Ocean and Indonesia). Indeed, in those cases we can firstly notice a peak of $h(500\text{hpa})$ over Africa from 10 to 30 days before the MJO triggering over Indian Ocean, in addition if we draw a line representing the MJO speed on a time-longitude diagram and if we extend this line backwards we reach the peak over Africa like in [fig 16](#), that means this burst of $h(500\text{hpa})$ is matching with the average propagation speed of the MJO with a week of uncertainty. We can also guess on the



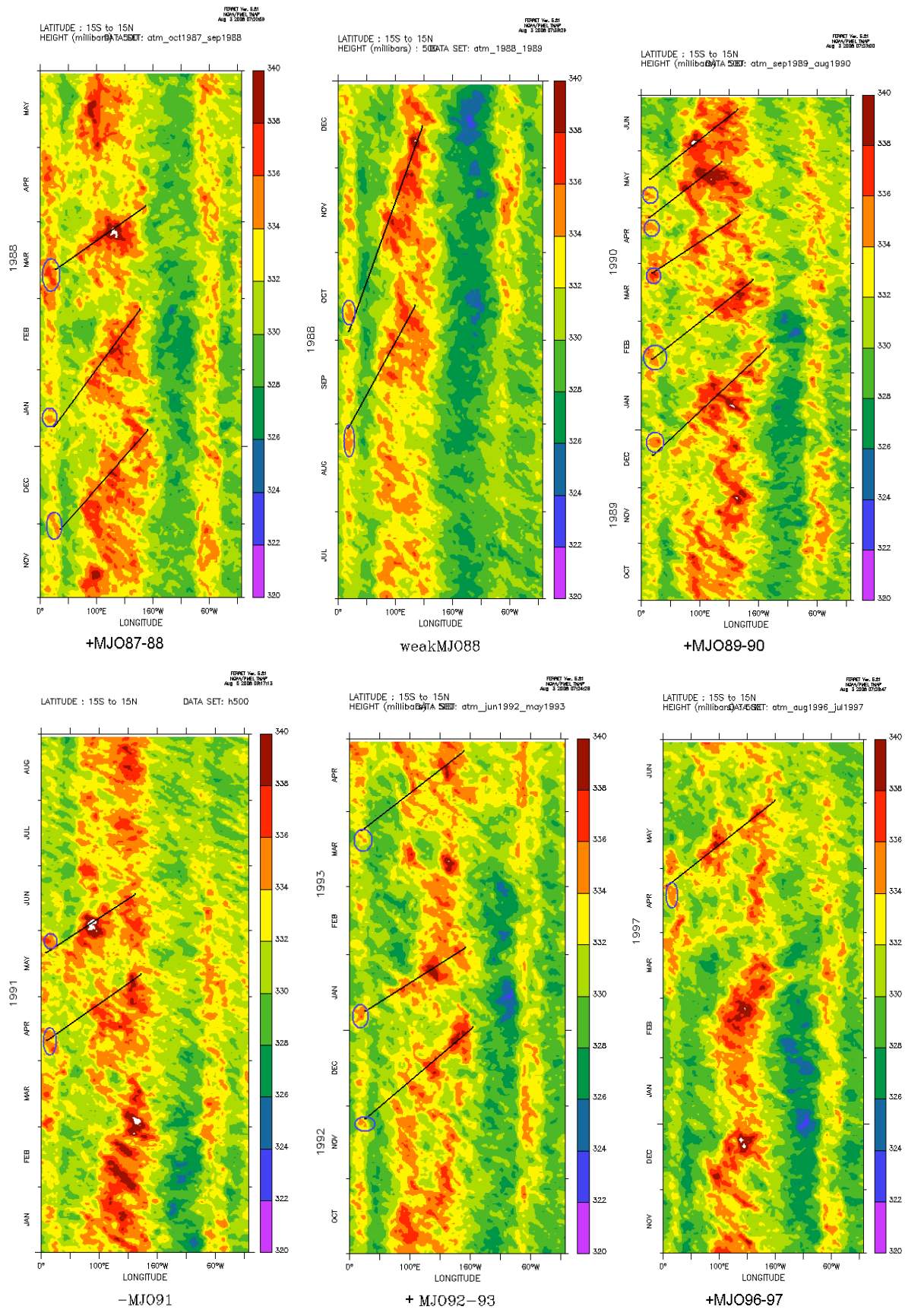


Figure 16 : Time-longitude diagrams of h (500hpa) averaged between 15°S-15°N for the 12 interesting cases. Black arrows draft the average speed of MJO, blue circles shows the possible corresponding peaks over Africa. Refer to table 1

corresponding diagrams that the periodicity of those burst is also matching sometimes with the MJO ones. Then in the next series (fig 16 and 17) of diagrams and plots, we display all the strong MJO events and weak MJO events listed in table 1. We noticed 12 interesting cases in a total of 18 where the correlation between the burst of h (500hpa) over Africa and the triggering of MJO (strong or weak) corresponds to the propagation speed of the wave, with one week of uncertainty. Moreover we noticed that 8 on 12 of those cases corresponds to strong MJOs. That let us suppose that in case of strong MJO, this plausible correlation between Africa and the two other regions is significantly better. Also in the time-series plots corresponding to each longitude-time diagrams, we see this kind of correlation between Africa and the two other regions.

The other 6 cases showed no obvious relations for being interpreted (fig18).

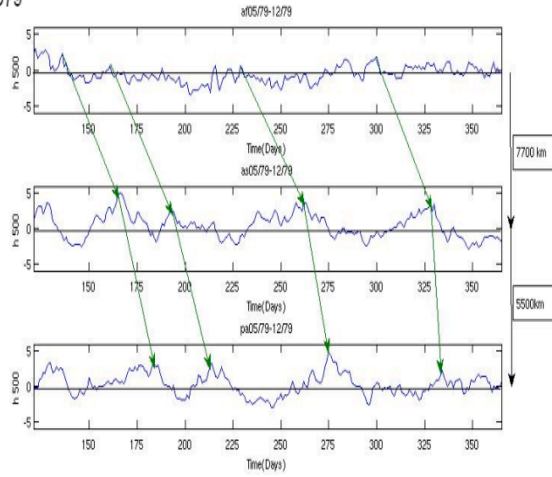
By doing the FFT transform and after normalisation by the red noise for every box we obtained the periodograms displayed in fig 19. Here we look for similarity in the spectral peaks, i.e events with same periodicity occur in all the 3 boxes, namely African box (called 'af'), Indian Ocean box (called 'as' like Asia) and eastern Indonesian box (called 'pa' like Pacific). We won't discuss the frequency similarity between Indian Ocean and Indonesia because they are well-known in any case of MJO strong or weak.

In those plots we have confronted each period-power (periodogram) normalized spectra for the nine couple Weak/Strong MJO we have sorted in the table 1. Considering that every peak over the 1,25 is significant (Hendon and Wheeler 2008) we have focused our attention on all the peaks situated within 20 days and 80 days period, knowing that the best range for observed **Tropical IntraSeasonal Variations (TISV)** periods is between 22 to 79 days (Masunaga 2007). Actually we don't focus our attention only on MJO (whose range is between 40 and 50 days), we extend our study of periodicity to the whole range of periods concerning the TISV in order to generalise our theory from the MJO to all the equatorial intraseasonal waves.

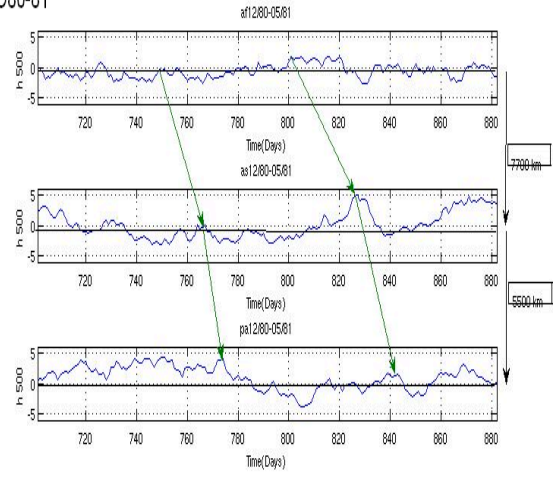
We notice that in case of weak MJO event there is strictly no good correlation between significant peaks in Africa and Asia or Africa and Pacific between 22 to 80 days period. However in case of strong MJO event for 5 cases on 9, we have such a correspondence between at least two regions and even sometimes between all of them. This result supports the hypothesis we made in part 3.2 about a possible better correspondence between the frequency profiles of those three regions when a strong MJO is there. Even if we are tempted to speak about a resonance profile, it's too early to conclude a resonance between Africa and the other two regions. It is implicitly meaning that the African signal of h (500hpa) leads the two other. However it opens this latter hypothesis about Africa as being the place where the wave could be initiated at least on some occasions. Such a hypothesis seems not to have been evoked yet in a paper. According to the statements of the part 2.3.f) we can suspect this connection might be lead by either a transport of moisture or a low pressure signal, and hence convective instability from African continent through Indian Ocean, due to the westerly 850hpa winds background flow prevailing over the equatorial Indian Ocean and Indonesian archipelago.

We can also see that in case of strong MJO events we have for 7 cases on 9 a significant peak for Africa in the [22-80 days] range against only 1 peak in the opposite case.

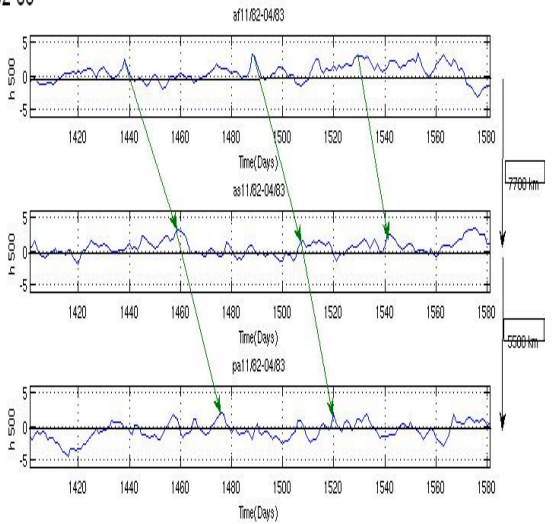
+MJO79



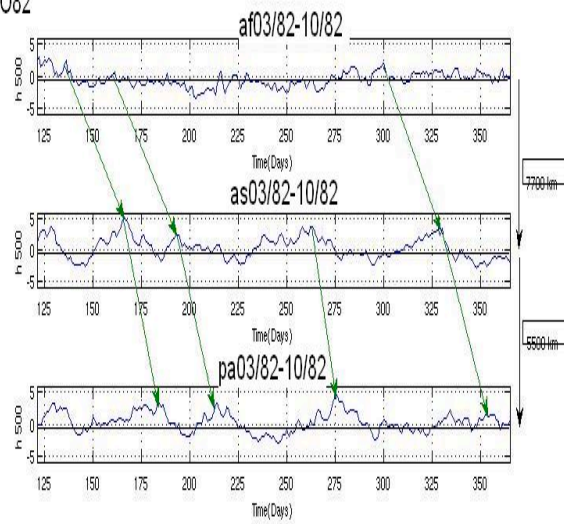
+MJO80-81



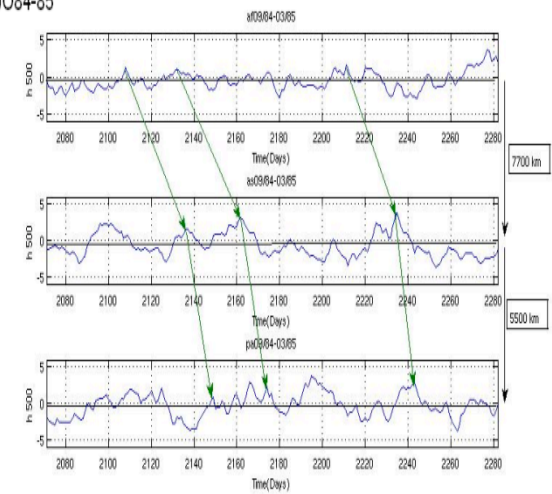
-MJO82-83



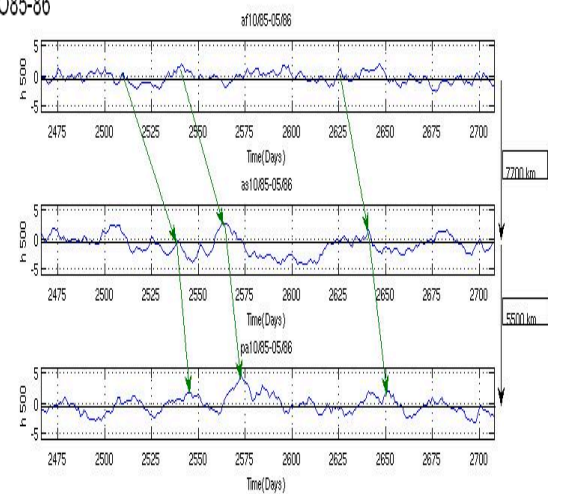
-MJO82



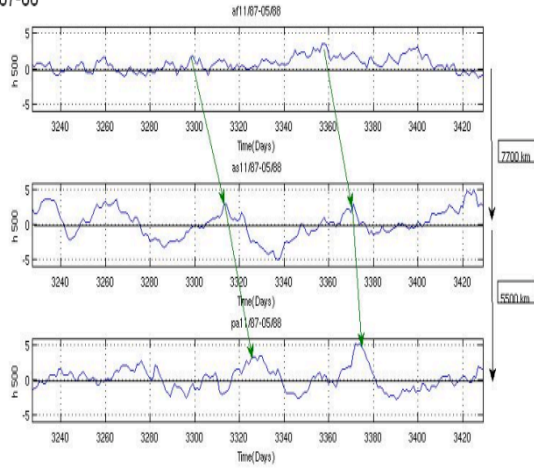
+MJO84-85



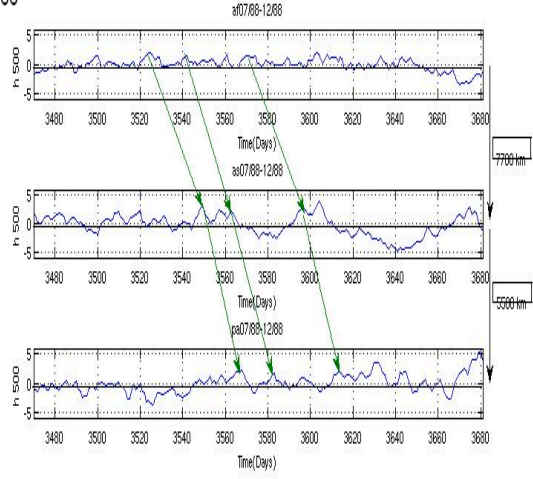
+MJO85-86



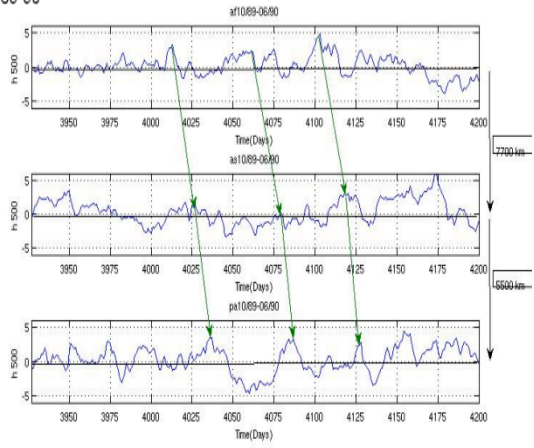
+MJO87-88



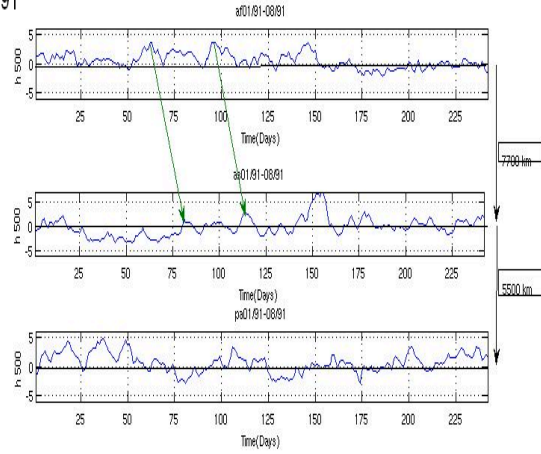
-MJO88



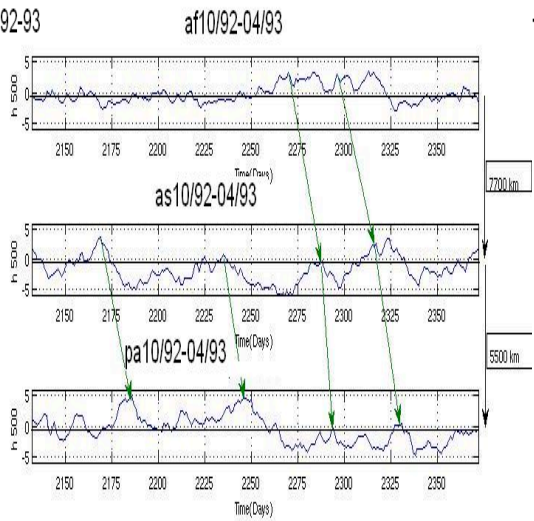
+MJO89-90



-MJO91



+MJO92-93



+MJO96-97

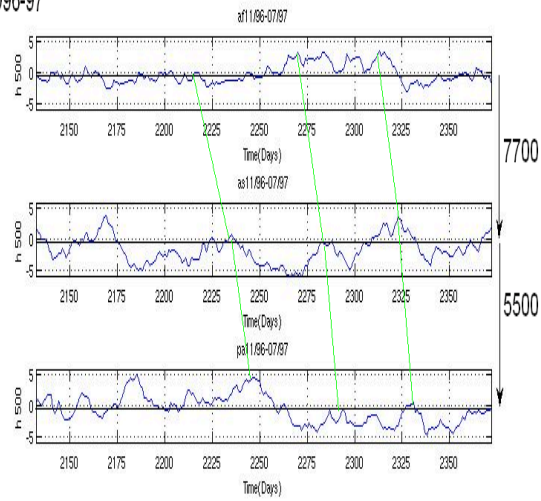


Figure 17 : Time-series of h (500hpa) averaged between 15°S-15°N corresponding to the previous diagrams, red arrows represents the hypothetical travelling of the wave from Africa (af) to Indian Ocean (Asia 'as') and Indonesia (Pacific 'pa').

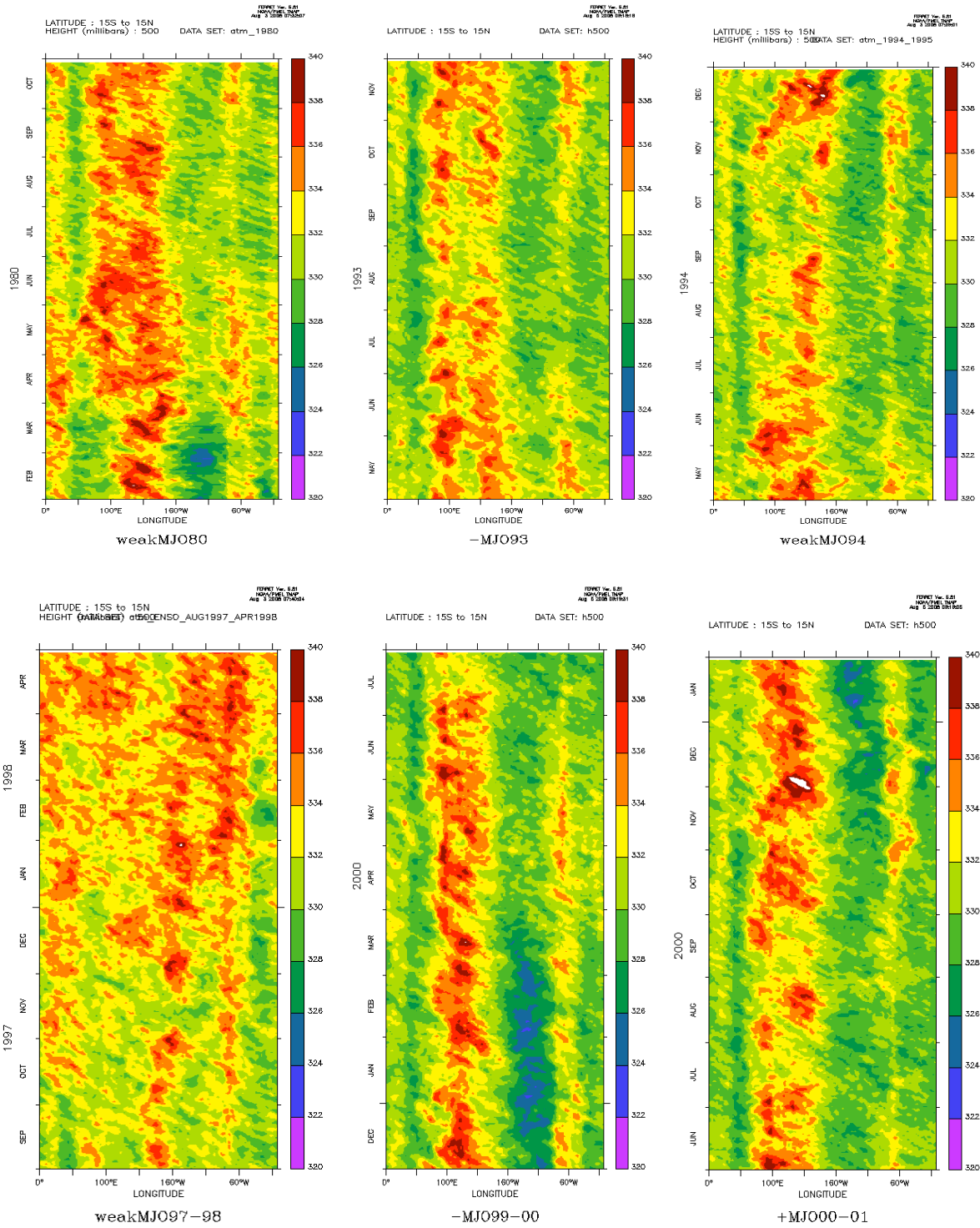
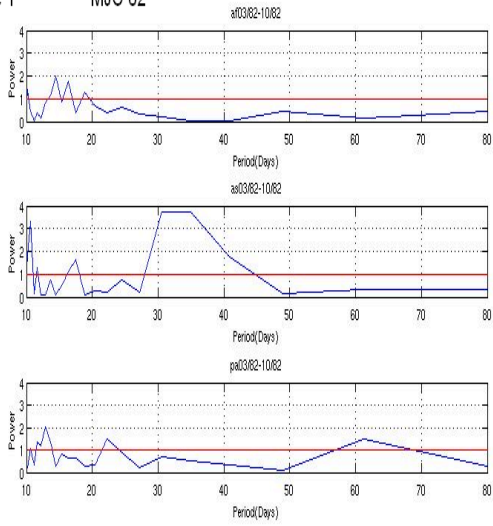
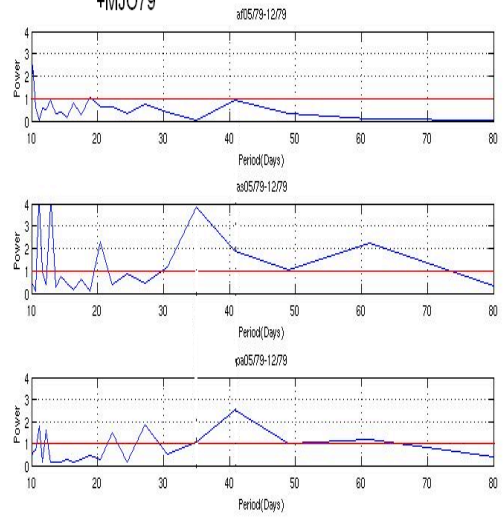


Figure 18 : Time-longitude diagrams of h (500hpa) averaged between 15°S-15°N for the 6 remaining events selected in the table 1 with a few or inexistent correlation between Africa's h (500hpa) fluctuations and MJO signal

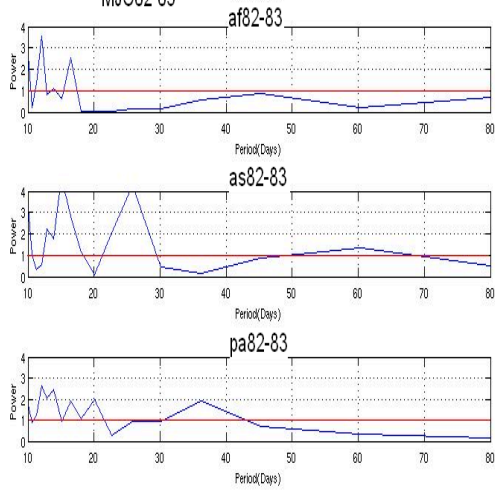
Couple 1 -MJO 82



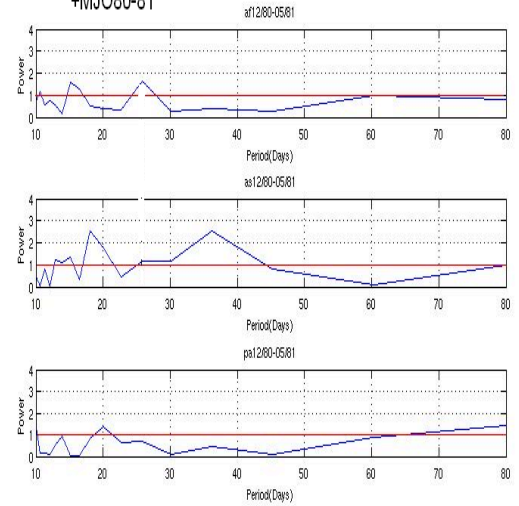
+MJO79



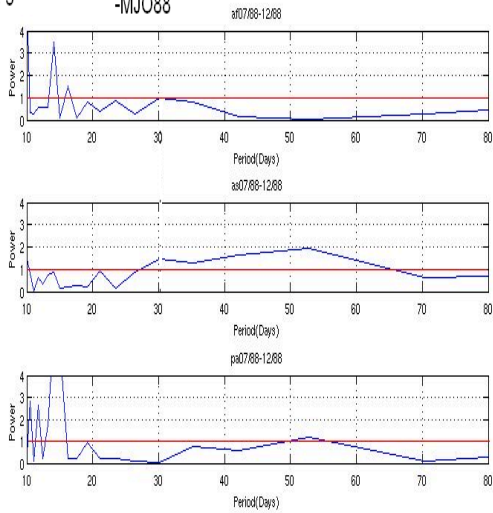
Couple 2 -MJO82-83



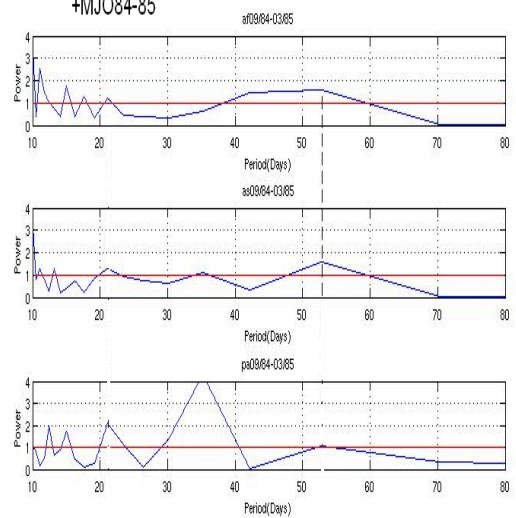
+MJO80-81



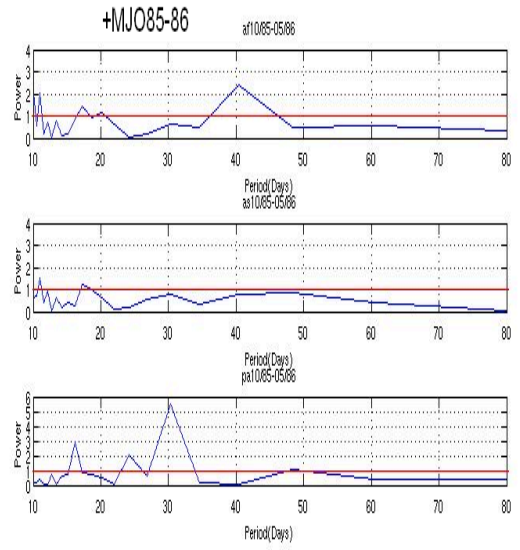
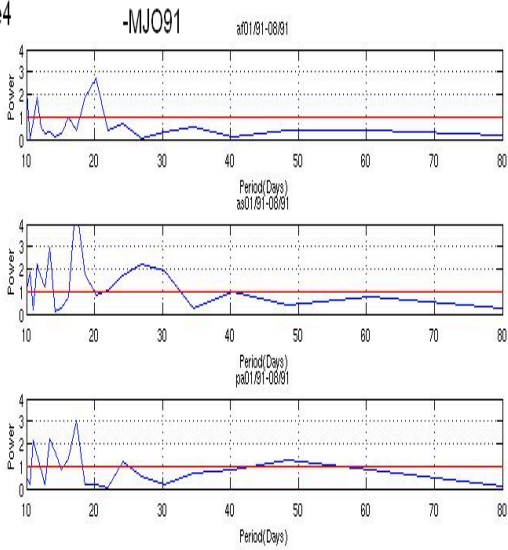
Couple 3 -MJO88



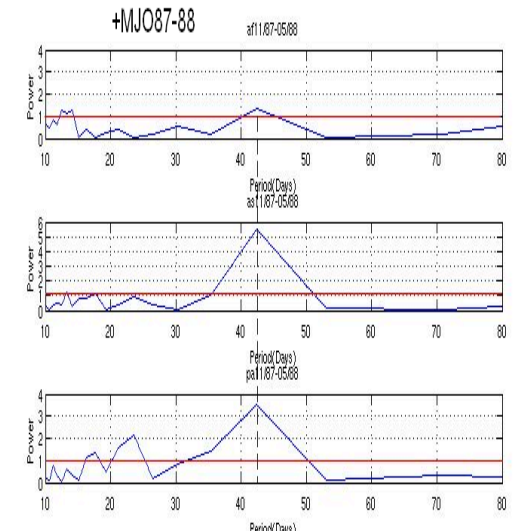
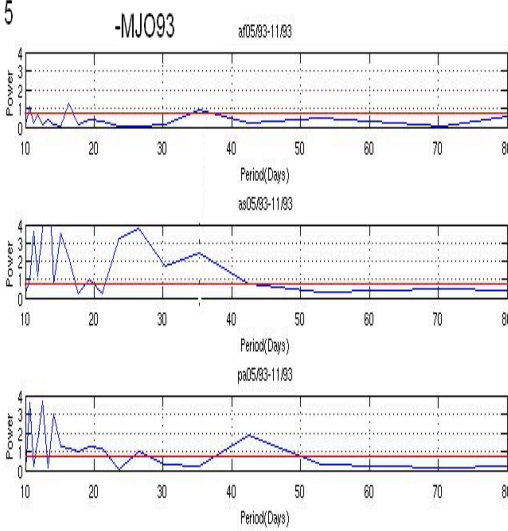
+MJO84-85



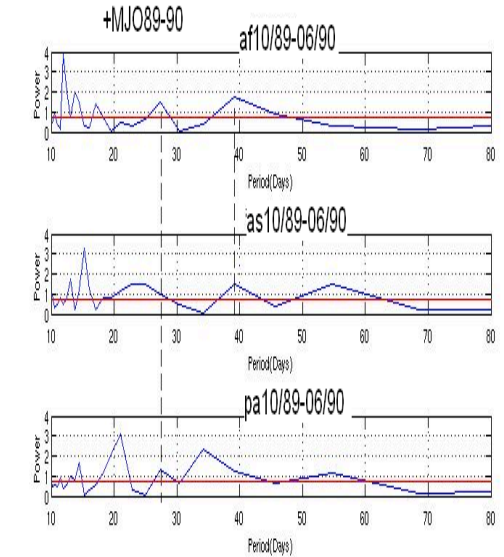
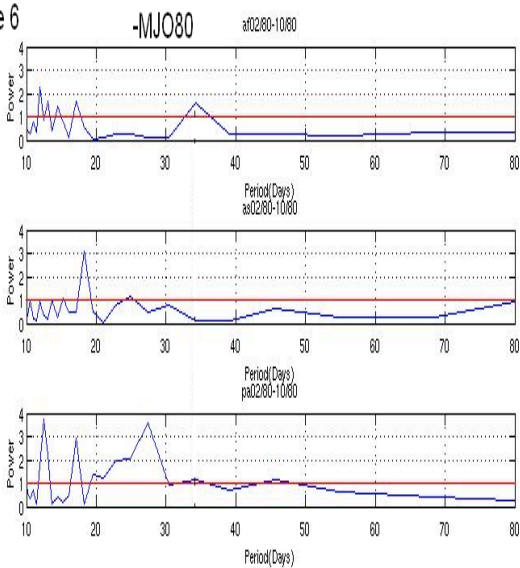
Couple 4



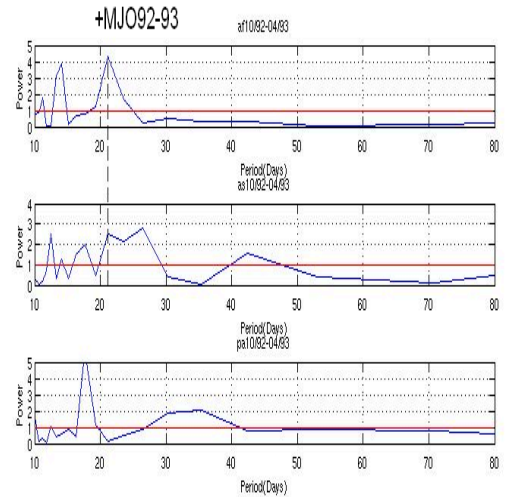
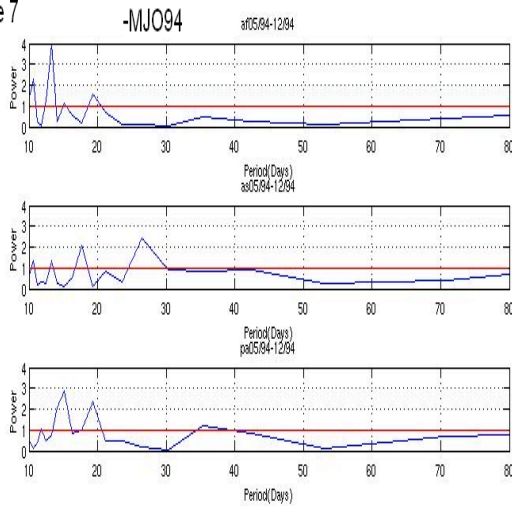
Couple 5



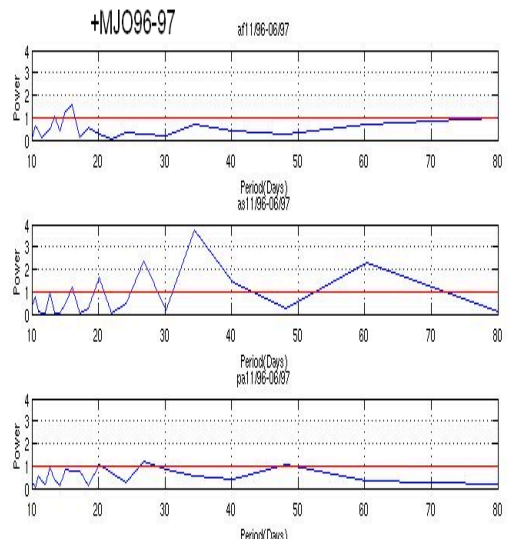
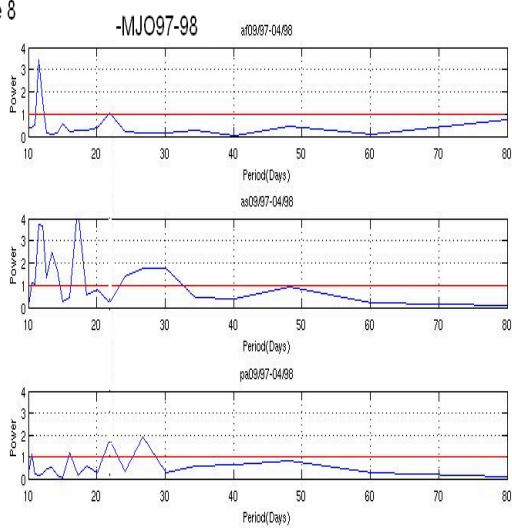
Couple 6



Couple 7



Couple 8



Couple 9

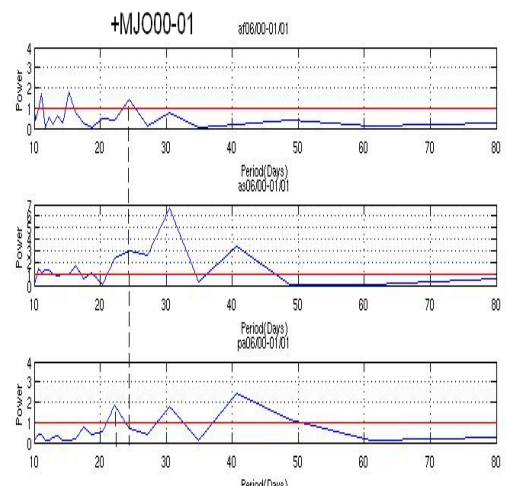
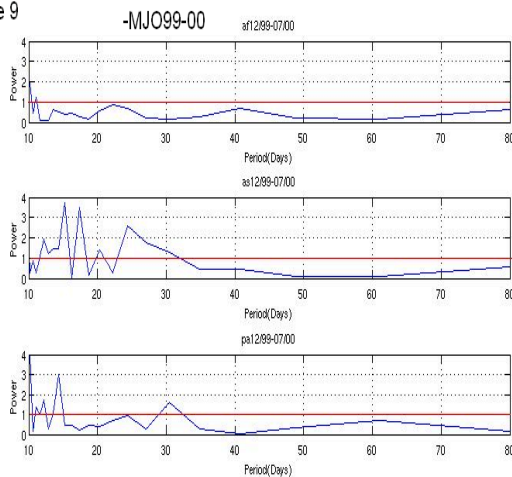


Figure 19: Period-Power spectrum for h(500hpa) averaged in Africa (upper plots) in Asia (middle plots) and Pacific (lower plots). Dotted line highlights period similarities between Africa and Asia, or Africa and Pacific, or the three for the peaks over 1.25. Red arrows display the red noise signal.

4. Concluding remarks

At the term of this study aimed to better understand the MJO by doing a comparative study between strong and weak MJO using h (500hpa) signal, we can make three main conclusions:

- The moist static energy at 500hpa can be a good proxy for studying the MJO signal. It has good correspondance in average speed, period, and propagation with OLR and 850hpa wind patterns which are the two typical proxies earlier used for tracking the MJO.
- Secondly we defined a westerly 850hpa winds background which might be the critical condition for the MJO eastward propagation. This westerly winds background could be maintained by the presence of strong deep convection zones during the summers of each hemisphere caused by a strong shortwave radiative forcing. One over northern Indian subcontinent during boreal summer, and the other one over northern Australia. Knowing that deep convection is correlated with large scale low sea level pressures those westerly near-to-surface westerly winds could be supposed as being geostrophic winds rounding around those two low pressure zones, and thanks to the Coriolis force, those wind remains eastward during the summers of each hemisphere.
- Finally by doing a short comparative spectral analysis between nine strong and nine weak MJO events, we conclude that it looks like the strengthen of MJO signal is partially correlated with the frequency coherence of the h (500hpa) signal over Africa, Indian Ocean and Western Indonesia although Africa is not recognized as being crossed by the OLR signal in MJO. Regarding only 18 statistical events (which is very few !), we had a frequency coherence:
 - 0% of the cases during weak MJO events
 - 56% of the cases during strong MJO events (5/9)

Then we can think about a possibility of an MJO starting in Africa and moving to Indian Ocean and in some cases with western Indonesia also. By combining the previous conclusion with this one, we can imagine either a transport of moisture from Africa to Indian Ocean or a pressure signal controlled by the westerly winds background or by a Kelvin wave which could trigger a deep convection event over it.

Nevertheless this hypothesis has to be confirmed by doing a better statistical analysis taking account of more number of strong and weak MJO and by using more accurate mathematical tools for wavelet filtering an analysis.

Acknowledgements

I first thank my professor **G-S Bhat** for his guidance and for accepting my candidature to realise my last year student project in the CAOS (Centre for Atmospheric and Oceanic Sciences, 560012 Bangalore, India). I thank also **Remy Roca** without whom I couldn't have done this project abroad. And also two PhD students by the name of **Sandeep Sahany** and **Saroj Kanta Mishra** for their helpful highlights and their friendship.

References

- *Hendon, Zhang, D.Glick*: “Interannual variations of the Madden-Julian Oscillations during Austral summer”, 1998, American Meteorological Society.
- *Hendon, Wheeler*: “An all-season multivariate MJO index”, 2004, American Meteorological Society.
- *Hendon, Wheeler*: “Some space-time spectral analysis of Tropical convection and planetary scale waves”, 2008, Journal of Atmospheric sciences.
- *Zhang*: “Madden-Julian Oscillations”, 2005, Review of Geophysics.
- *Torrence and Compo*: “A practical guide to wavelet analysis”, 1998, American Meteorological Society
- *Masunaga*: “Seasonality and regionality of the Madden-Julian Oscillations, Kelvin Wave, and equatorial Rossby wave”, 2007, American Meteorological Society